Received: 15 September 2021 | Revised: 18 November 2021 | Accepted: 23 November 2021

DOI: 10.1002/cne.25283

RESEARCH ARTICLE

JCN RESEARCH IN SYSTEMS NEUROSCIENCE THE JOURNAL OF COMPARATIVE NEUROLOGY WILEY

Local olfactory interneurons provide the basis for neurochemical regionalization of olfactory glomeruli in crustaceans

Steffen Harzsch[1,2] | **Heinrich Dircksen**[3] | **Bill S. Hansson**[2]

[1] Department of Cytology and Evolutionary Biology, Zoological Institute and Museum, University of Greifswald, Greifswald, Germany

[2] Department of Evolutionary Neuroethology, Max-Planck-Institute for Chemical Ecology, Jena, Germany

[3] Department of Zoology, Stockholm University, Stockholm, Sweden

Correspondence
Steffen Harzsch, Department of Cytology and Evolutionary Biology, Zoological Institute and Museum, University of Greifswald, Soldmannstrasse 23, D-17498 Greifswald, Germany.
Email: steffen.harzsch@uni-greifswald.de

Funding information
DFG, Grant/Award Number: Ha 2540/19-1; Max Planck Society

Abstract

The primary olfactory centers of metazoans as diverse as arthropods and mammals consist of an array of fields of dense synaptic neuropil, the olfactory glomeruli. However, the neurochemical structure of crustacean olfactory glomeruli is largely understudied when compared to the insects. We analyzed the glomerular architecture in selected species of hermit crabs using immunohistochemistry against presynaptic proteins, the neuropeptides orcokinin, RFamide and allatostatin, and the biogenic amine serotonin. Our study reveals an unexpected level of structural complexity, unmatched by what is found in the insect olfactory glomeruli. Peptidergic and aminergic interneurons provide the structural basis for a regionalization of the crustacean glomeruli into longitudinal and concentric compartments. Our data suggest that local olfactory interneurons take a central computational role in modulating the information transfer from olfactory sensory neurons to projection neurons within the glomeruli. Furthermore, we found yet unknown neuronal elements mediating lateral inhibitory interactions across the glomerular array that may play a central role in modulating the transfer of sensory input to the output neurons through presynaptic inhibition. Our study is another step in understanding the function of crustacean olfactory glomeruli as highly complex units of local olfactory processing.

KEYWORDS
Coenobita clypeatus, Crustacea, neuropeptides, olfactory glomeruli, olfactory interneurons, olfactory system, *Pagurus bernhardus*

1 | INTRODUCTION

In the brains of mice (Imai, 2014; Mombaerts, 2006; Sinakevitch et al., 2017; Takeuchi & Sakano, 2014), insects (e.g., Fuscà & Kloppenburg, 2021; Galizia, 2014; Galizia & Rössler, 2010; Hansson & Anton, 2000; Martin et al., 2011; Szyszka & Galizia, 2015) and malacostracan crustaceans (Derby & Weissburg, 2014; Harzsch & Krieger, 2018; Sandeman et al., 2014; Schachtner et al., 2005; Schmidt & Mellon, 2011), the primary olfactory centers consist of an array of fields of dense synaptic neuropil, the olfactory glomeruli. These fundamental units of olfactory processing are sites where axons from olfactory sensory neurons synapse with local olfactory interneurons and olfactory projection neurons. In malacostracan crustaceans, the afferent input to the glomeruli is provided by olfactory sensory neurons housed in aesthetascs, specialized, unimodal olfactory sensilla on the deutocerebral antennal pair (Derby et al., 2016; Hallberg & Skog, 2011; Schmidt & Mellon, 2011). Acetylcholine likely represents the main transmitter of the olfactory sensory neurons (Schachtner et al., 2005)

but the afferents also contain orcokinin-like neuropeptides (Polanska et al., 2020). In basal lineages of malacostracan crustaceans, the olfactory glomeruli are spherical but in lineages with more sophisticated olfactory systems, they take on an elongate shape (Harzsch & Krieger, 2018). Within the primary olfactory centers, represented by the bilaterally paired, deutocerebral olfactory lobes, the glomeruli are radially arranged around the periphery of a core of non-synaptic fibers, the projection neuron hub (Polanska et al., 2020), in a highly geometrical constellation (Figure 1a–c; reviews Derby & Weissburg, 2014; Harzsch & Krieger, 2018; Sandeman et al., 2014; Sandeman & Mellon, 2002; Schachtner et al., 2005; Schmidt & Mellon, 2011).

Crustacean glomeruli of the elongate type typically are regionalized into functional compartments along their long axis, and in representatives of the crayfish (Blaustein et al., 1988; Sandeman & Luff, 1973), clawed lobsters (Langworthy et al., 1997), spiny lobsters (Blaustein et al., 1988; Schmidt & Ache, 1992, 1996, 1997; Wachowiak et al., 1997; Wachowiak & Ache, 1997), and hermit crabs (Harzsch & Hansson, 2008; Krieger et al., 2010, 2012), an outer cap, a subcap, and a base region can be distinguished (Figure 1d). This regionalization is also mirrored in the glomerular neurochemistry (Langworthy et al., 1997; Polanska et al., 2012, 2020; Schmidt & Ache, 1997) and has functional implications. The termination pattern of the olfactory sensory neuron afferents within the glomeruli was most thoroughly analyzed in crayfish and spiny lobsters (Blaustein et al., 1988; Mellon & Alones, 1993; Sandeman & Luff, 1973; Sandeman & Sandeman, 1994; Schmidt & Ache, 1992). The axons form a distal layer around the periphery of the lobe, which is frequently described as a plexus and from which axon bundles segregate and enter the glomeruli at right angles to the surface of the lobe (Tuchina et al., 2015). The projection pattern of the afferents in crayfish appears to be nontopographic (Mellon & Alones, 1993) in that axons from a cluster of olfactory sensory neurons associated with one aesthetasc sensillum target many glomeruli of the lobe (Mellon & Munger, 1990; Sandeman & Denburg, 1976). In spiny lobsters and hermit crabs, most of the afferent axons terminate densely within the cap region of the glomeruli, making this area the major input region (Schmidt & Ache, 1992; Tuchina et al., 2015). However, in both groups, some axons also project down the entire length of the glomeruli into the subcap and base regions.

Within the glomeruli, the afferents engage in synaptic interactions with local olfactory interneurons and olfactory projection neurons, which provide an output channel to the lateral protocerebrum (Figure 1c,e; reviews Derby & Weissburg, 2014; Sandeman et al., 2014; Sandeman & Mellon, 2002; Schachtner et al., 2005; Schmidt, 2007; Schmidt & Mellon, 2011). This study will focus on the local olfactory interneurons that innervate the glomeruli. These neurons can be broadly subdivided into two morphological classes, one of which primarily targets the cap and subcap regions of the glomeruli ("rim" interneurons), and a second class, which primarily invades the base of the glomeruli from inside of the lobe ("core" interneurons; Schachtner et al., 2005; Schmidt & Ache, 1996; Wachowiak et al., 1997). However, local interneurons display a considerable diversity in their morphology and additional types exist that cannot be classified in the two mentioned classes (Schachtner et al., 2005). Local olfactory interneurons also display a large diversity in their neurochemistry (see Table 1). "Core" interneurons were shown to possess neuroactive substances as diverse as nitric oxide, serotonin, histamine, and FMRFamide-related peptides (FaRPs) (Schachtner et al., 2005), whereas "rim" interneurons contain GABA (Schachtner et al., 2005), FaRPs, and allatostatins (Polanska et al., 2012) as well as orcokinin (Polanska et al., 2020).

The present study sets out to enhance our understanding of the neurochemical basis of glomerular regionalization in two crustacean representatives, *Coenobita clypeatus* and *Pagurus bernhardus* (Malacostraca, Anomala), where, in previous studies, we have described highly complex central olfactory systems with several hundreds of olfactory glomeruli (Harzsch & Hansson, 2008; Krieger et al., 2012; Polanska et al., 2012, 2020; Tuchina et al., 2015). To that end, we explored the neurochemical diversity of local olfactory interneurons using sets of antisera against three neuropeptides and a biogenic amine, combined with immunolocalization of presynaptic vesicle proteins.

2 | MATERIALS AND METHODS

2.1 | Immunohistochemistry

Immunohistochemistry was carried out on free-floating vibratome sections (80 μm) of brains from adult specimens as previously described in detail for *Pagurus bernhardus* (Anomala, Paguridae; Krieger et al., 2012) and *Coenobita clypeatus* (Anomala, Coenobitidae; Harzsch & Hansson, 2008; Polanska et al., 2012, 2020). Adult and sexually mature males of *P. bernhardus* were obtained from the animal supply unit of the Alfred Wegener Institute at Helgoland (https://www.awi.de/ueber-uns/standorte/helgoland/service/biologischer-materialversand.html) where the animals were reared in flow-through systems with seawater from their natural habitat and ambient light conditions. Adult males of *C. clypeatus* (Herbst, 1791; Anomura, Coenobitidae) were obtained from the "Zoologischer Großhandel Peter Hoch" (August Jeanmaire Str. 12, 79183 Waldkirch, Germany). Upon receipt, all animals were immediately processed and anaesthetized by placing them on crushed ice prior to decapitation and dissection of the brain. The following antisera were used for double labeling experiments:

- Monoclonal mouse anti-synapsin "SYNORF1" antibody (RRID: AB_2315426; final dilution 1:30; antibody provided by E. Buchner, Universität Würzburg, Germany),
- Polyclonal rabbit anti-A-type Dipallatostatin I, APSGAQRLYGFGLamide, (Jena Bioscience, abd-062; RRID: AB_2314318; final dilution 1:1,000),
- Monoclonal mouse-anti allatostatin I/AST7 antibody 5F10, APSGAQRLYGFGLamide (Stay et al., 1992; RRID:AB_528076; final dilution 1:100; Developmental Studies Hybridoma Bank; https://dshb.biology.uiowa.edu/5F10),
- Polyclonal rabbit anti-FMRFamid (RRID AB_572232; final dilution 1:2,000; ImmunoStar; cat. No. 20091, Lot No. 923602),
- Polyclonal rabbit anti-orcokinin (final dilution 1:200; RRID: AB_2315017 (Bungart et al., 1994; Dircksen et al., 2000),

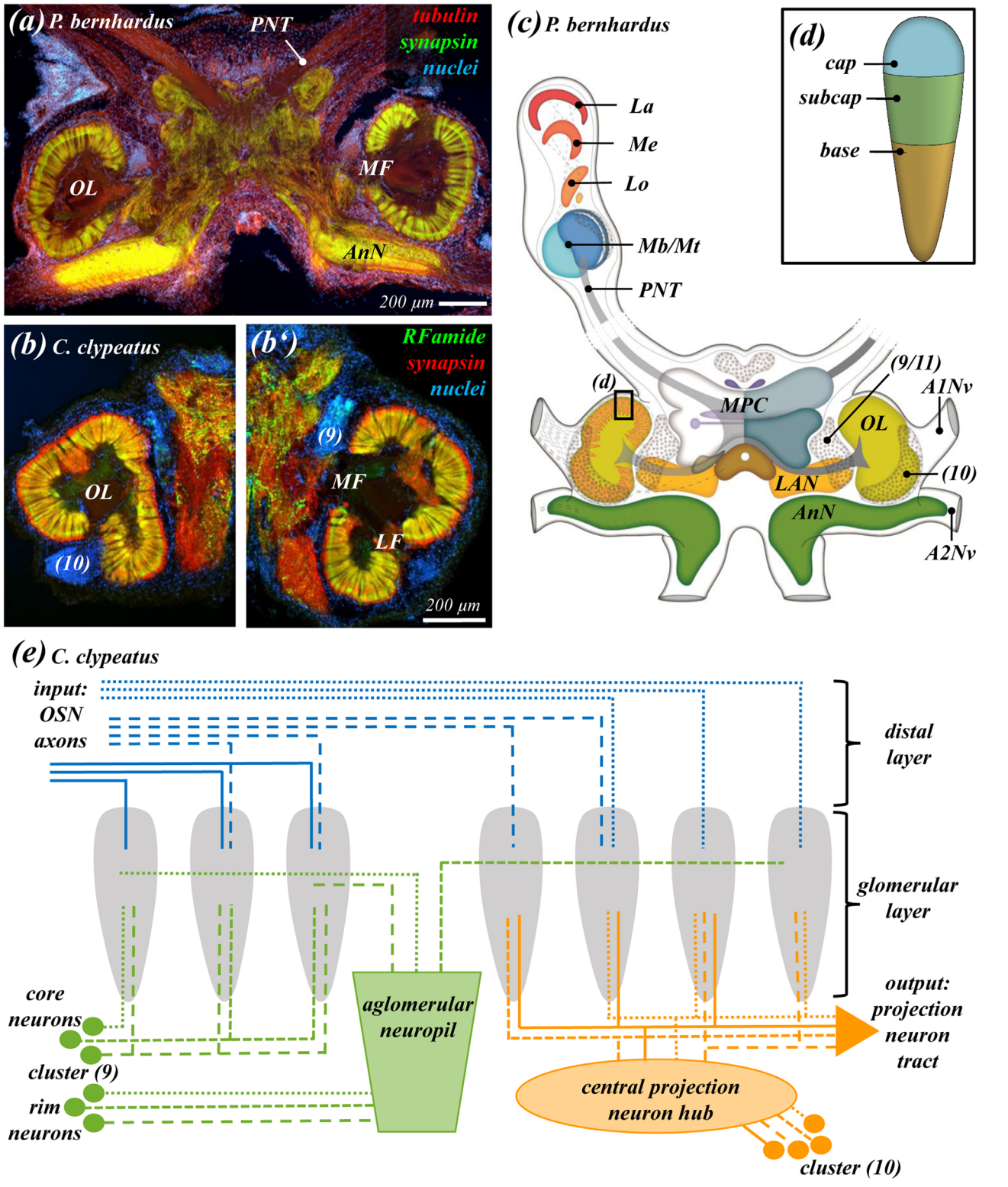

FIGURE 1 (a) Horizontal brain section of *Pagurus bernhardus* at low magnification showing the bilaterally arranged olfactory lobes (modified from Krieger et al., 2012). (b, b') Horizontal brain sections (left and right hemispheres at different z levels) of *Coenobita clypeatus* at low magnification (modified from Harzsch & Hansson, 2008). (c) Scheme of the brain in *P. bernhardus* (modified from Krieger et al., 2012; boxed area identifies the location of (d)). (d) Olfactory glomeruli in hermit crabs are subdivided in cap, subcap, and base compartments (modified from Polanska et al., 2012). (e) Model summarizing the innervation of the olfactory glomeruli in *C. clypeatus* with afferents, local olfactory interneurons, and olfactory projection neurons (modified from Polanska et al., 2020). Abbreviations: AnN, antenna 2 neuropil; A1Nv, A2Nv antenna 1 and 2 nerves; La, lamina; LAN, lateral antennular neuropil; Lf, lateral foramen; Mb/Mt, mushroom body and medulla terminalis; Me, medulla; Mf, median foramen; MPC, medial protocerebrum; Lo, lobula; OL, olfactory lobe; OSN, olfactory sensory neuron; PNT, projection neuron tract; (9/11), (10); cell clusters (9/11) and (10)

TABLE 1 Neurochemistry of local olfactory interneurons in selected crustaceans

Spiny lobster (Achelata)	
serotonin	(Schmidt & Ache, 1997)
GABA	(Orona et al., 1990; Wachowiak et al., 1997; Wachowiak & Ache, 1997)
Dopamine	(Schmidt & Ache, 1994, 1997)
Histamine	(Orona & Ache, 1992; Wachowiak & Ache, 1997)
FaRPs	(Schmidt, 1997b; Schmidt & Ache, 1994, 1997)
SCP_B	(Schmidt & Ache, 1997)
Substance P	(Schmidt & Ache, 1994, 1997)
Clawed lobster (Homarida)	
Serotonin	(Beltz et al., 1990; Beltz, 1999; Helluy et al., 1993; Langworthy et al., 1997)
Histamine	(Langworthy et al., 1997)
Nitrid oxide	(Benton et al., 2007; Scholz et al., 1998)
Dopamine	(Schmidt, 1997a)
FaRPs	(Kobierski et al., 1987)
SCPB	(Langworthy et al., 1997)
Substance P	(Langworthy et al., 1997)
Crayfish (Astacida)	
Serotonin	(Mellon & Alones, 1993; Sandeman et al., 1988, 1995; Sandeman & Sandeman, 1994, 1987)
Nitric oxide	(Johansson & Mellon, 1998)
Enkephalin	(Ollivaux, 2002, p. 2)
FaRPs	(Yasuda-Kamatani & Yasuda, 2006)
TRP	(Johansson et al., 1999; Yasuda-Kamatani & Yasuda, 2006)
Allatostatin	(Yasuda-Kamatani & Yasuda, 2006)
Orcokinin	(Yasuda-Kamatani & Yasuda, 2006)
Substance P	(Sandeman et al., 1990; Schmidt, 1997b)
Hermit crabs (Anomala)	
Serotonin	(Harzsch & Hansson, 2008; Polanska et al., 2020), and present report
TH	(Kotsyuba, 2012)
FaRPs	(Harzsch & Hansson, 2008; Krieger et al., 2012; Polanska et al., 2012; Schachtner et al., 2005), and present report
Allatostatin	(Harzsch & Hansson 2008, Krieger et al. 2010, 2012, Polanska et al. 2012), and present report
SIFamide	(Krieger et al., 2010)
Orcokinin	(Polanska et al., 2020), and present report
Substance P	(Schmidt, 1997b)
True crabs (Brachyura)	
Serotonin	(Antonsen & Paul, 2001; Johansson, 1991; E. Kotsyuba & Dyachuk, 2021; Krieger et al., 2010, 2015)
ChAT	(Kotsyuba & Dyachuk, 2021)
Nitric oxide	(Kotsyuba et al., 2010; Kotsyuba & Dyachuk, 2021)
FaRPs	(Kotsyuba & Dyachuk, 2021)
GnRH	(Saetan et al., 2013)
Allatostatin	(Krieger et al., 2010, 2015)
Proctolin	(Wood et al., 1996)
Substance P	(Schmidt, 1997b)

Abbreviations: ChAT, cholin acetyltransferase; FaRPs: FMRFamide-related peptides, GABA, γ–aminobytric acid; GnRH: gonadotropin-releasing hormone-like peptides; SCPB, small cardioactive peptide B; TH, tyrosine hydroxylase; TRP, tachykinin-related peptide

- Polyclonal rabbit anti-serotonin (RRID: AB_572263; final dilution 1:1.000; ImmunoStar Incorporated; cat. No. 20080, lot No. 541016),
- Secondary reagents: Alexa Fluor 488-conjugated goat anti-rabbit IgG Antibody (final dilution 1:1,000; Invitrogen, Thermo Fisher Scientific; Waltham, MA, USA; RRID: AB_10374301); Cy3-conjugated AffiniPure goat anti-mouse IgG Antibody (final dilution 1:1,000; Jackson ImmunoResearch Laboratories Inc.; West Grove, PA, USA; RRID: AB_2338000).

In control experiments, we replaced the primary antisera with phosphate buffered saline in which case all staining was abolished. Successfully processed sections were analyzed using a Zeiss LSM 700 meta confocal microscope. Digital images were processed with Adobe Photoshop CS4 or ImageJ. Only global picture enhancement features (brightness and contrast) were used to adjust images. Our analysis is based on more than 10 successfully processed brains per marker set, and the labeling pattern was consistent between these specimens.

2.2 | Primary antibody characterization

2.2.1 | Synapsin

The monoclonal anti-SYNORF1 synapsin antibody (DSHB Hybridoma Product 3C11; anti SYNORF1 as deposited to the DSHB by E. Buchner, University Hospital Würzburg, Germany; supernatant) was raised against a *Drosophila melanogaster* GST-synapsin fusion protein and recognizes at least four synapsin isoforms (70, 74, 80, and 143 kDa) in western blots of *D. melanogaster* head homogenates (Klagges et al., 1996). Sullivan et al. (2007) mention a single band at approximately 75 kDa in a western blot analysis of crayfish brain homogenate. Harzsch and Hansson (2008) conducted a western blot analysis comparing brain tissue of *D. melanogaster* and the hermit crab *C. clypeatus*. The SYNORF1 serum provided identical results for both species, and it stained one strong band between 80 and 90 kDa and a second weaker band slightly above 148 kDa, suggesting that the epitope that SYNORF1 recognizes is strongly conserved between *D. melanogaster* and *C. clypeatus* (Harzsch & Hansson, 2008). Similar to the fruit fly, the antibody consistently labels brain structures in other major subgroups of the malacostracan crustaceans (e.g., Beltz et al., 2003; Harzsch et al., 1998, 1999; Harzsch, 2002; Krieger et al., 2012) in a pattern that is consistent with the assumption that this antibody labels synaptic neuropils in crustaceans.

2.2.2 | Allatostatin A-like peptides

The A-type allatostatins (A-ASTs; synonym Dip-allatostatins) constitute a large family of neuropeptides that were first identified from the cockroach *Diploptera punctata* and that share the C-terminal motif–YXFGLamide (Nässel & Homberg, 2006; Stay & Tobe, 2007). In decapod crustaceans, almost 20 native A-ASTs and related peptides were initially identified from extracts of the thoracic ganglia of the shore crab *Carcinus maenas* (Duve et al., 2002) and shortly after several other A-ASTs were isolated from the freshwater crayfish *Orconectes limosus* (Dircksen et al., 1999). Meanwhile, the family of crustacean A-ASTs has substantially grown to several dozens of representatives (Christie et al., 2010), with additional members being discovered, for example, in the prawns *Penaeus monodon* (Duve et al., 2002) and *Macrobrachium rosenbergii* (Yin et al., 2006), in the brachyuran crab *Cancer borealis* (Huybrechts et al., 2003), the crayfish *Procambarus clarkii* (Yasuda-Kamatani & Yasuda, 2006), the lobster *Homarus americanus* (Cape et al., 2008), the shrimp *Litopenaeus vannamei* (Christie, 2014), and nonmalacostracan crustaceans such as the copepod *Calanus finmarchicus* (Christie et al., 2008) and representatives of the genus *Daphnia* (Dircksen et al., 2011; Kress et al., 2016). Yasuda-Kamatani and Yasuda (2006) have shown that more than 25 closely related ASTA-like peptides occur on the same crayfish *P. clarkii* allatostatin-like peptide precursor, and could thus be coreleased. Christie (2016) predicted a total of 29 peptides with the C-terminal motif, -YXFGLamide, in the latest bioinformatic analysis on the peptidome of the shore crab *C. maenas*.

The 5F10 monoclonal mouse anti-allatostatin I/AST7 antiserum that we used was raised against synthetic AST 7 (APSGAQRLYGFGL), N-terminal coupled to bovine serum albumin (BSA) using glutaraldehyde (Stay et al., 1992; Woodhead et al., 1992). In ELISA essay, 5F10 was shown to be two to three orders of magnitude more sensitive to APSGAQRLYGFGLamide than to other allatostatins (Stay et al., 1992). This antiserum most likely binds to all A-ASTs that share the typical C-terminal -XFGLamide motif. This antiserum was widely used to analyze elements of the nervous system in the cockroach *D. punctata* (Stay et al., 1992; Woodhead et al., 1992), the vinegar fly *D. melanogaster* (Yoon & Stay, 1995) as well as the brachyuran crab *Neohelice* (*Chasmagnathus*) *granulata* (Maza et al., 2016), and the copepod *C. finmarchicus* (Christie et al., 2008; C. H. Wilson & Christie, 2010). To confirm the specifity of 5F10 antiserum in crustaceans, in a study on *C. finmarchicus* the primary antibody was preadsorbed with 10^{-5} M APSGAQRLYGFGLamide for 2 h at room temperature prior to its application to tissue (Christie et al., 2008). We also used an antiserum that was raised against the *D. punctata* (Pacific beetle cockroach) A-type Dipallatostatin I, APSGAQRLYGFGLamide, coupled to bovine thyroglobulin using glutaraldehyde (Vitzthum et al., 1996) that was kindly provided by H. Agricola (Friedrich-Schiller Universität Jena, Germany) and that has previously been used to localize A-ASTs in crustacean and insect nervous systems (e.g., Dircksen et al., 1999; Kreissl et al., 2010; Utting et al., 2000; Vitzthum et al., 1996) including *C. clypeatus* and *P. bernhardus* (Harzsch & Hansson, 2008; Krieger et al., 2012; Polanska et al., 2012). Competitive ELISA with Dip-allatostatin I, II, III, IV, and B2 showed that the antiserum is two orders of magnitudes more sensitive to Dip-allatostatin I than to Dip-allatostatins II, III, IV, and B2 (Vitzthum et al., 1996). Furthermore, the antiserum displays no cross-reactivity with corazonin, CCAP, FMRFamide, leucomyosuppression, locustatachykinin 11, perisulfakinin, and proctolin as tested by non-competitive ELISA. Preadsorption of the diluted antisera against Dip-allatostatin I abolished all immunostaining in the brain sections of *Schistocerca gregaria* (Vitzthum et al., 1996). A sensitive competitive enzyme immunoassay (EIA) confirmed the high specificity of the antiserum for A-type Dip-allatostatin I (Dircksen et al., 1999). In the brains of the honey bee *Apis mellifera*, preadsorption controls with AST I and AST VI

completely abolished all staining of the antiserum (Kreissl et al., 2010). Sombke et al. (2011) repeated a preadsorption test in the centipede *Scutigera coleoptrata* and preincubated the antiserum with 200 μg/ml A-type allatostatin I (Sigma, A9929; 16 h 4°C), and this preincubation abolished all staining. Preadsorption of the antiserum with AST-III was reported to abolish all labeling in the stomatogastric nervous system of the crab *Cancer pagurus*, the lobster *H. americanus* and the crayfish *Cherax destructor*, and *P. clarkii* (Skiebe, 1999). This antiserum most likely binds to all A-ASTs that share the typical C-terminal -XFGLamide motif. However, the term "allatostatin A-like immunoreactivity" is used throughout this study for labeling with both the monoclonal and polyclonal antiserum because it may be possible that these antibodies also bind related peptides.

2.2.3 | FMRFamide-like peptides

The tetrapeptide FMRFamide and FMRFamide-related peptides (FaRPs) are prevalent among invertebrates and vertebrates and form a large neuropeptide family with more than 50 members all of which share the RFamide motif (Dockray, 2004; Nässel & Homberg, 2006; Zajac & Mollereau, 2006). In malacostracan Crustacea, at least 12 FaRPs have been identified and sequenced from crabs, shrimps, lobsters, and crayfish (Huybrechts et al., 2003; Mercier et al., 2003), which range from seven to 12 amino acids in length and most of which share the carboxyterminal sequence Leu-Arg-Phe-amide. The utilized antiserum was generated in rabbit against synthetic FMRFamide (Phe-Met-Arg-Phe-amide) conjugated to bovine thyroglobulin. According to the manufacturer, immunohistochemistry with this antiserum is completely eliminated by pretreatment of the diluted antibody with 100 μg/ml of FMRFamide. Harzsch and Hansson (2008) repeated this experiment in the anomuran *C. clypeatus*, and preincubated the antiserum with 100 μg/ml FMRFamide (Sigma; 16 h, 4°C) resulting in a complete abolishment of all staining. Because the crustacean FaRPs known so far all share the carboxyterminal sequence LRFamide, we conclude that the DiaSorin antiserum that we used most likely labels any peptide terminating with the sequence RFamide. Therefore, we will refer to the labeled structures in our specimens as "RFamide-like immunoreactivity" throughout the study.

2.2.4 | Orcokinin

The first orcokinin was discovered almost 3 decades ago in extracts (Stangier et al., 1992) and later in neurons of the abdominal nerve cord of the crayfish *Orconectus limosus* (Astacida; Dircksen et al., 2000). Yasuda-Kamatani and Yasuda (2000, 2006) identified two different orcokinin gene products in the crayfish *P. clarkii* showing that the cloned mRNA precursors gave rise to multiple copies of the first discovered and name-giving Asn^{13}-orcokinin but also to single copies of another four isoforms with modified C-terminal or internal amino acids; all orcokinin-isoforms were also identified biochemically in this study. At present, orcokinins are known to represent a highly conserved family of neuropeptides identified in many crustacean and insect species (Bungart et al., 1994; Hofer et al., 2005; Hofer & Homberg, 2006a, 2006b). In crustaceans, these neuropeptides are widely distributed in the nervous system and display strong myotropic and neuromodulatory activities (Bungart et al., 1994, 1995; Dircksen et al., 2000; L. Li et al., 2002). In most of the hitherto investigated insects, orcokinins are one amino acid longer (14 amino acids) and may play different roles than in crustaceans. Experiments on the cockroach *Leucophaea maderae* proved that orcokinins are engaged in the regulation of locomotor activity controlled by circadian clock neurons (Hofer & Homberg, 2006a). In the silk moth *Bombyx mori*, orcokinins were described as neuronal prothoracicotropic factors regulating the biosynthesis of ecdysteroids (Yamanaka et al., 2011). Recently, by use of transcriptome shotgun assembly (TSA) data sets, orcokinin-encoding transcripts were predicted in spiders (Christie & Chi, 2015), and, by immunocytochemistry, orcokinin-immunoreactive neurons were identified in ticks (Ladislav et al., 2015). We used a rabbit anti-Asn^{13}-orcokinin (Asn^{13}-OK) antiserum (Bungart et al., 1994) that was raised against a glutaraldehyde-conjugate of bovine thyroglobulin and Asn13-OK and already applied in a previous study on *C. clypeatus* (Polanska et al., 2020). Most likely because of the very conserved N-terminal sequence NFDEIDR- in most orcokinins discovered to date, the Asn^{13}-OK-antiserum showed almost full cross-reaction with Val^{13}-orcokinin (Dircksen et al., 2000) and likely all other C-terminally modified crustacean and even identified insect (cockroach *Rhyparobia = Leucophaea maderae*) orcokinins (Hofer et al., 2005) showing this C-terminal sequence.

2.2.5 | Serotonin

The antiserum against serotonin is a polyclonal rabbit antiserum raised against serotonin coupled to BSA with paraformaldehyde. The antiserum was quality control tested by the manufacturer using standard immunohistochemical methods. According to the manufacturer, staining with the antiserum was completely eliminated by pretreatment of the diluted antibody with 25 μg of serotonin coupled to BSA per milliliter of the diluted antibody. We repeated this control with the serotonin-BSA conjugate that was used for generation of the antiserum as provided by ImmunoStar (cat. No. 20081, lot No. 750,256; 50 μg of lyophilized serotonin creatinine sulfate coupled to BSA with paraformaldehyde). Preadsorption of the antibody in working dilution with the serotonin-BSA conjugate at a final conjugate concentration of 10 μg/ml at 4°C for 24 h completely blocked all immunolabeling. We performed an additional control and preadsorbed the diluted antiserum with 10 mg/ml BSA for 4 h at room temperature. This preadsorption did not affect the staining, thus providing evidence that the antiserum does not recognize the carrier molecule alone. The manufacturer also examined the cross-reactivity of the antiserum. According to the data sheet, with 5 μg, 10 μg, and 25 μg amounts, the following substances did not react with the antiserum diluted to 1:20,000 using the horse radish peroxidase (HRP) labeling method: 5-hydroxytryptophan, 5-hydroxyindole-3-acetic acid, and dopamine. We previously used this

antiserum to detect serotonin-immunoreactive neurons in the brain of *C. clypeatus* (Harzsch & Hansson, 2008).

3 | RESULTS

The olfactory lobes (OL) are bilaterally paired brain centers (Figure 1a–c). In the following plates, the left column of images shows the left OL of *P. bernhardus*, and the right column, the right OL of *C. clypeatus*. We will call the entire array of glomeruli the "glomerular layer" (GL) in the following as introduced in our previous report (Polanska et al., 2020). The GL surrounds a nonsynaptic fibrous core (FC). There are also a few patches of non-glomerular synaptic neuropil, which are identified by single letters according to the nomenclature established in Harzsch and Hansson (2008). We will focus our description on the local olfactory neurons, the somata of which are located in cell clusters (9) and (11) in the terminology of Sandeman et al. (1992). The neurites of these interneurons enter the lobe via a gap in the GL, called the median foramen (MF, Harzsch and Hansson 2008, Polanska et al. 2020) and target the glomeruli from the inside of the lobe.

3.1 | Marker set 1: Synapsin-immunoreactivity (syn-ir) and serotonin-immunoreactivity (5HT-ir)

3.1.1 | Pagurus bernhardus

Two types of local olfactory interneurons with serotonin-immunoreactivity (5HT-ir) are present in the deutocerebrum of this species (Figure 2a,b), one class with smaller somata in cell cluster (9) and another with larger somata in cell cluster (11). Both extend neurites into the center of the lobe (asterisk in Figure 2b) but unfortunately, we could not disentangle if the two types have different projection patterns. Neurites with 5HT-ir target the base of the glomeruli within the glomerular layer from the proximal side (Figures 2c and 3b). The base and subcap areas of the glomeruli are filled with a loose network of 5HT-ir neurites, whereas little labeling is present in the cap region (Figures 2c and 3a,b). This network is also visible in cross-sections of the glomeruli at the subcap level (Figure 3c,d).

Synapsin-immunoreactivity (syn-ir) is present across the entire glomerular volume (Figures 2c and 3a). This signal appears stronger in the glomerular subcap region. In fact, syn-ir is also present in the interglomerular space between the subcap regions of neighboring glomeruli (arrows in Figures 2c and 3a). This syn-ir has a coarse, granular appearance, and displays a signal that is stronger than that within the glomerular volume. The interglomerular synaptic profiles are also visible in cross-sections of the glomeruli (arrows in Figure 3d; see also Figure 12).

3.1.2 | Coenobita clypeatus

Smaller local olfactory interneurons, which display 5HT-ir, are located in cell cluster (9) (Figure 2d), and larger ones in cell cluster (11) (data not shown; compare Harzsch & Hansson, 2008). A bundle of strongly immunolabeled neurites (asterisk in Figure 2e) from cluster (9) enters the center of the lobe via the medial foramen (mF), where it splits into an anterior (aB) and a posterior (pB) bundle (Figure 2d). Neurites from these bundles enter the base of the glomeruli (asterisk in Figure 2f) to fill the glomerular base and subcap regions with a network of immunolabeled fibers, whereas the cap region itself is devoid of labeling (Figure 2f). Conspicuous, rod-shaped areas of dense 5HT-ir material are present within the center of the subcap of each glomerulus (double arrowheads in Figures 2f and 3e). These areas are also visible in cross-sections of the subcap region (Figure 3g,h). In many glomeruli, it appears that two of the rod-shaped profiles in neighboring glomeruli stem from a single bundle of 5HT-ir neurites (Figure 3e,f). We will refer to these as "rod domains" (single) and "fork domains." Cross-sections reveal that the fork domains link pairs of glomeruli (Figure 3g,h; see also Figure 12). Such cross-sections reveal a considerable variability in glomerular diameters across the glomerular array. We did not encounter any interglomerular synaptic profiles as in *P. bernhardus* (Figure 3g,h).

3.2 | Marker set 2: Serotonin-immunoreactivity (5HT-ir) and allatostatin-like immunoreactivity (AST-ir)

3.2.1 | Pagurus bernhardus

Within cluster (9), somata displaying allatostatin-like immunoreactivity (AST-ir) are located in close vicinity to those with 5HT-ir (Figure 4a,b). The glomerular layer shows a particularly strong AST-ir signal in its distal part (Figure 4a). Higher magnification of individual glomeruli shows that the label is particularly dense in the subcap region, whereas the base is filled with a loose network of labeled fibers (Figures 4c and 5a). From the subcap, rod-shaped extensions protrude into the cap region. We will refer to these extensions as "baton domains" (more detailed description in the next section; see also Figure 12). Cross-sections at the level of the base region show both signals of 5HT-ir and AST-ir dispersed across the diameter of the neuropil (Figure 5b). Higher magnifications reveal that there is not any overlap of these two populations of neurites within the base region (Figure 5c).

3.2.2 | Coenobita clypeatus

Within cluster (9), somata displaying AST-ir are strictly separated from those with 5HT-ir in that a cluster of somata with AST-ir appears to be surrounded by a group of neurons with 5HT-ir. This population of AST-ir somata that belong to the "rim" type was already described in Polanska et al. (2012), a study in which we estimated their number to at least one hundred per side. There seem to be many more neurons of both AST-ir and 5HT-ir neurons than in *P. bernhardus* (Figure 4e). The glomerular layer shows a particularly strong AST-ir signal around its periphery (Figure 4d,e; compare also Polanska et al., 2012, 2020).

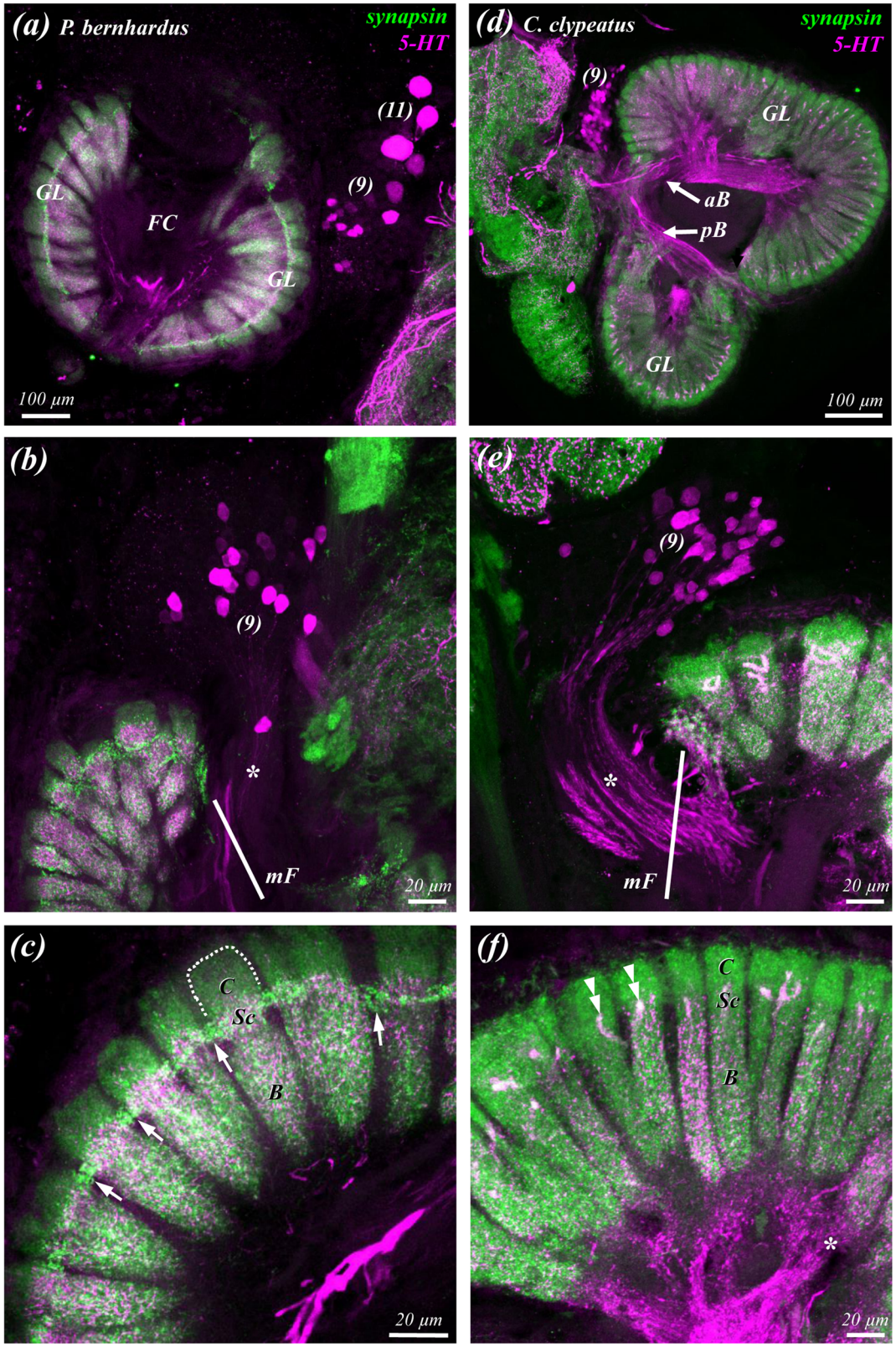

FIGURE 2 Synapsin-immunoreactivity (green) and serotonin-immunoreactivity (magenta) in horizontal sections of the olfactory deutocerebrum of *P. bernhardus* (a–c, left column, showing the left olfactory lobe) and *C. clypeatus* (d–f, right column, showing the right olfactory lobe). Anterior is toward the top. For explanation of asterisks, arrows, and arrowheads, see related text. Abbreviations: aB, anterior bundle; B, base; C, cap; GL, glomerular layer; FC, fibrous core; mF, median foramen; pB, posterior bundle; Sc, subcap; (9), (11) cell clusters (9) and (11)

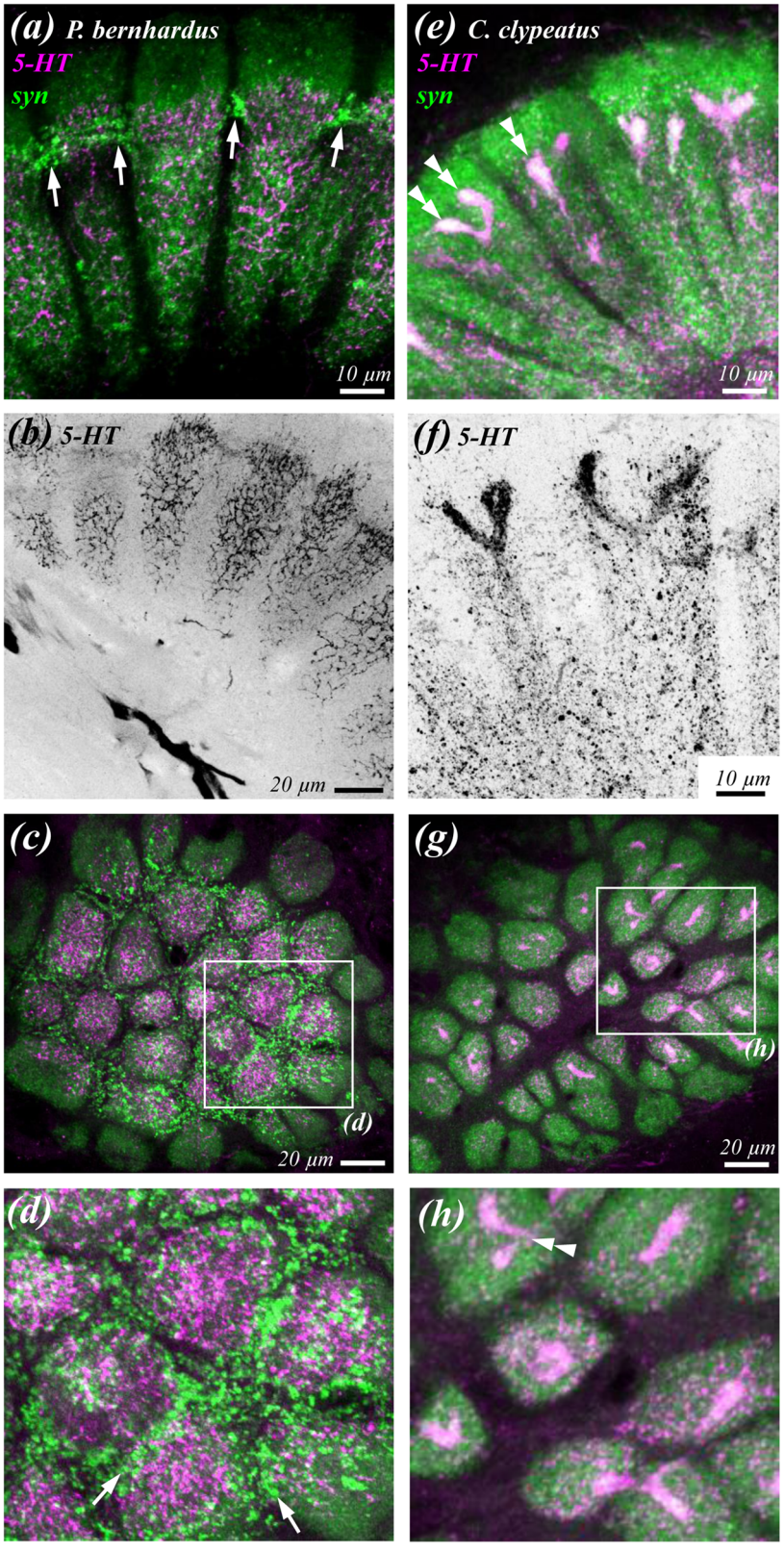

FIGURE 3 Synapsin-immunoreactivity (green) and serotonin-immunoreactivity (magenta) in the olfactory glomeruli of *P. bernhardus* (a–d, left column) and *C. clypeatus* (e–h, right column). (b and f)were black-white inverted. (a and b) and (e and f) longitudinal sections of the glomeruli, and (c and d) and (g and h) transverse sections of the subcap area. For explanation of arrows and arrowheads, see related text

As reported in Polanska et al. (2012), the axons of these interneurons penetrate into the olfactory lobe via the mF in a massive bundle which splits up to target the olfactory glomeruli and gives rise to strong immunoreactivity in these (Figures 4d and 8c,d). These authors and Polanska et al. (2020) described that AST-ir axon bundles do not target the base of the glomeruli, but rather that the axon bundles penetrate the glomerular array to then spread out tangentially to form a tangential belt of interglomerular fibers which laterally connects multiple glomeruli at the subcap level (Figures 6e and 8e and 12; and see the next section). Polanska et al. (2012) also described a second type of

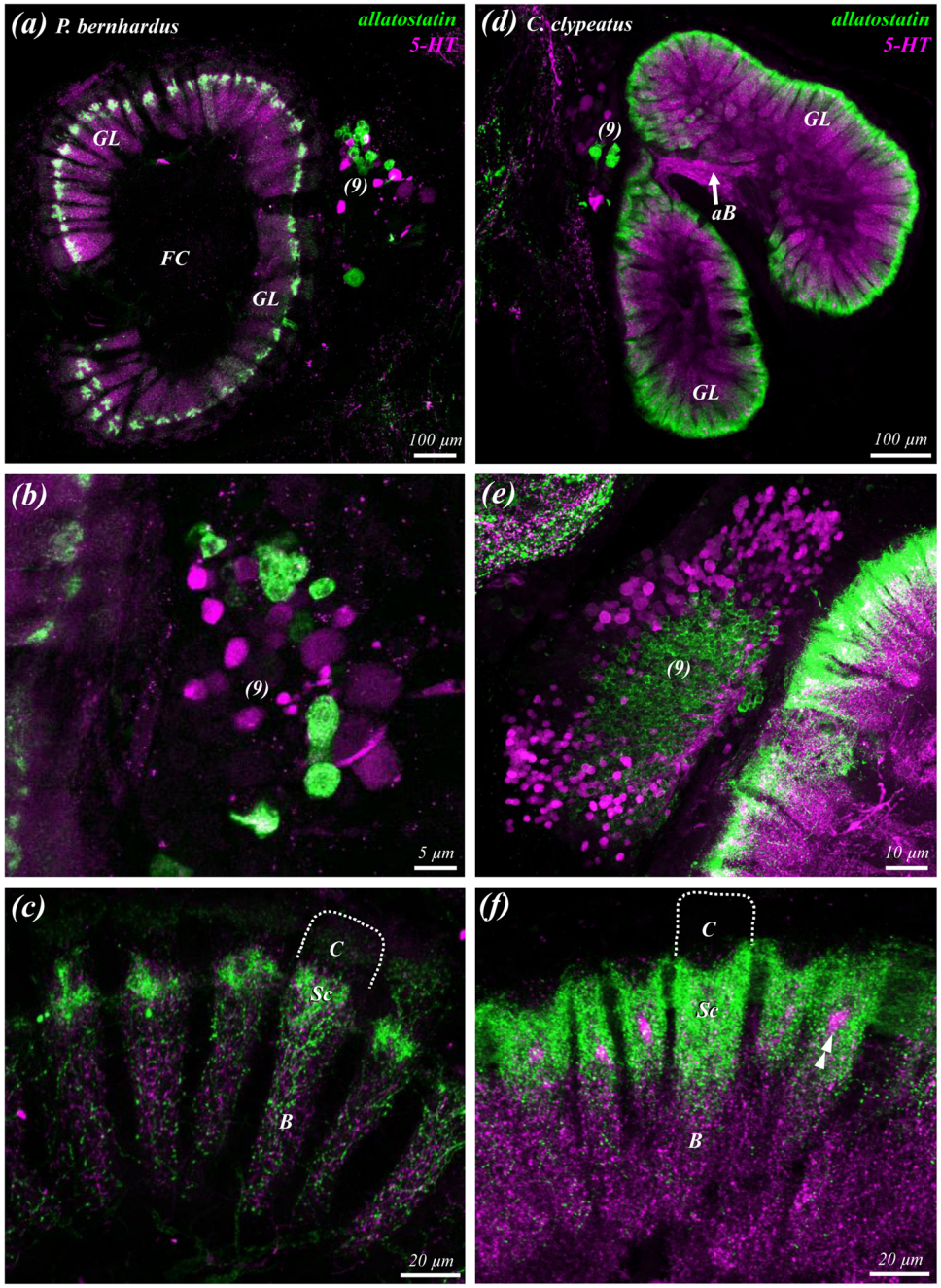

FIGURE 4 Allatostatin-like immunoreactivity (green) and serotonin-immunoreactivity (magenta) in horizontal sections of the olfactory deutocerebrum of *P. bernhardus* (a–c, left column, showing the left olfactory lobe) and *C. clypeatus* (d–f, right column, showing the right olfactory lobe). Anterior is toward the top. For explanation of arrowheads, see related text. Abbreviations: aB, anterior bundle; B, base; C, cap; GL, glomerular layer; FC, fibrous core; mF, median foramen; Sc, subcap; (9) cell cluster (9)

AST-ir neurons, with their somata located in cluster (11) and axons that do not penetrate into the core of the OL as the types described above, but spread around the outside of the olfactory lobe (Figure 12).

Higher magnifications reveal a dense plexus of immunolabeled neurites in the subcap region, which distally has a concave surface and which we will call "beaker domain" in the following (Figures 4f and 5d). These beaker domains surround the rod domains and fork domains of 5HT-ir material (double arrowheads in Figure 4f). There are not any domains with AST-ir of the baton type as seen in *P. bernhardus*. Cross-sections clearly visualize the spatial relationships of beaker domains and the rod/fork domains (Figure 5e, and double arrowheads in Figure 5f). Such cross-sections at the subcap level also reveal weakly AST-ir material between the glomeruli (arrows in Figure 5f; see also Figure 7g) and again show a considerable variability in the shape of glomerular cross-sections and their diameter across the glomerular array.

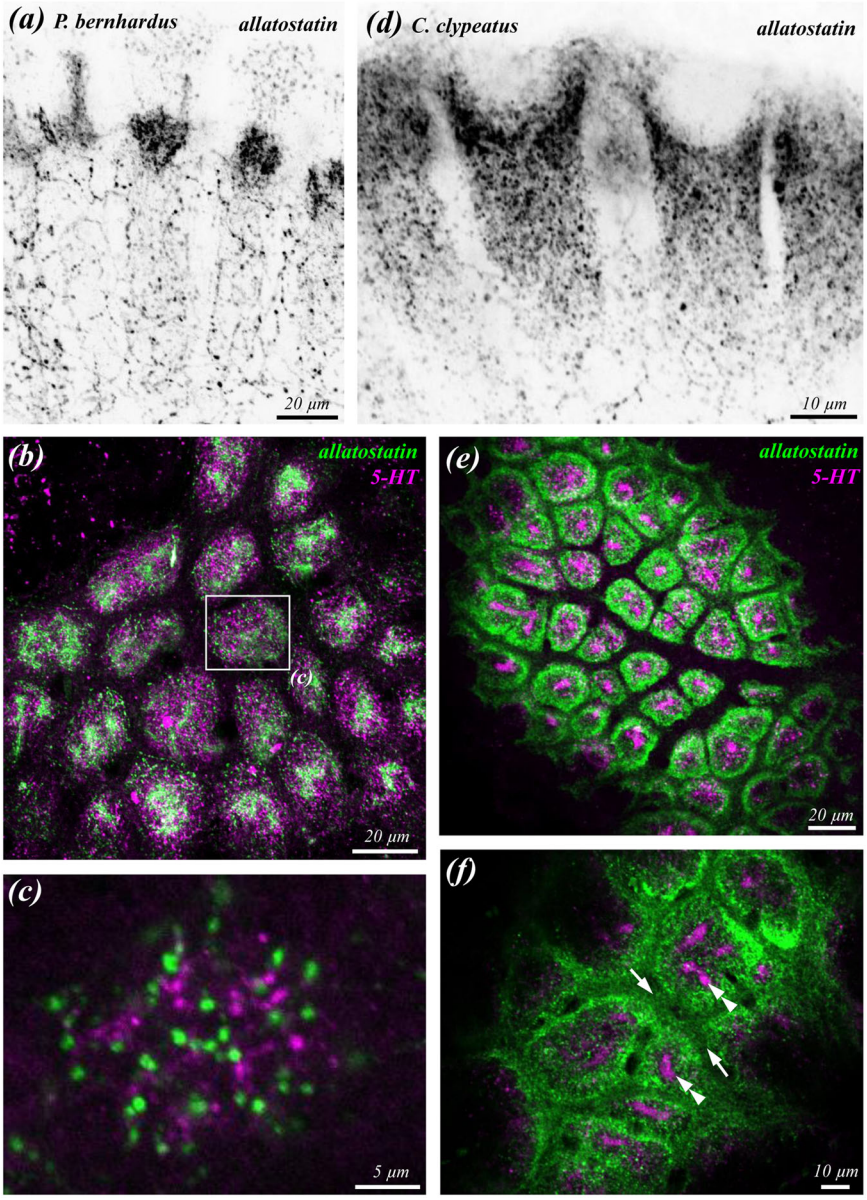

FIGURE 5 Allatostatin-like immunoreactivity (green and black) and serotonin-immunoreactivity (magenta) in the olfactory glomeruli of *P. bernhardus* (a–c, left column) and *C. clypeatus* (d–f, right column). (a) and (d) were black-white inverted. (a) and (d) are longitudinal sections of the glomeruli, and (b and c) and (e and f) transverse sections of the subcap area. For explanation of arrows and arrowheads, see related text

3.3 | Marker set 3: Allatostatin-like immunoreactivity (AST-ir) and RFamide-like immunoreactivity (RF-ir)

3.3.1 | Pagurus bernhardus

Somata displaying RFamide-like immunoreactivity (RF-ir) are located in close vicinity to those with AST-ir and both types include somata of different sizes (Figure 6a,b). Within the glomerular layer of the olfactory lobe, the strongest labeling for RF-ir is located in the periphery in low power magnifications (Figures 6a and 8b). The neurites of RF-ir somata in cluster (9) enter the lobe via the mF and seem to enter the base of the glomeruli from the proximal side of the glomerular layer (Figure 8b). Higher magnifications of the glomeruli show a dense labeling in the subcap region. At the level of the interface between the subcap and base regions, a bundle of RF-ir neurites horizontally links multiple glomeruli (arrows in Figure 6c and 7c; see also Figure 12). Interglomerular fibers with strong RF-ir are also visible in tangential sections of the glomerular layer at the subcap level (Figure 7a,b). Within the volumes of the glomeruli, RF-ir and AST-ir material shows little or no colocalization in the same profiles (Figure 7b).

Cluster 9 interneurons with AST-ir also seem to target the proximal part of the glomerular layer (Figures 6b and 9a,b). Higher magnifications of the glomerular subcap region again show a strong labeling of AST-ir material in the subcap (Figure 9a,b) and the characteristic baton domains extending into the cap region, as mentioned in the previous section (double arrowheads in Figure 7c–e). Furthermore, in these images, profiles with AST-ir are visible in the cap region as small dots (Figure 7c,e). In black-white inverted images that exclusively show the signal of AST-ir, these dots are visible more clearly (Figure 9c,d). Higher magnifications show that the profiles seem to be positioned at somewhat regular intervals and that they show a granular texture (Figure 9e). Even higher magnifications show that the profiles represent round fields of labeled material that appear as dots of different

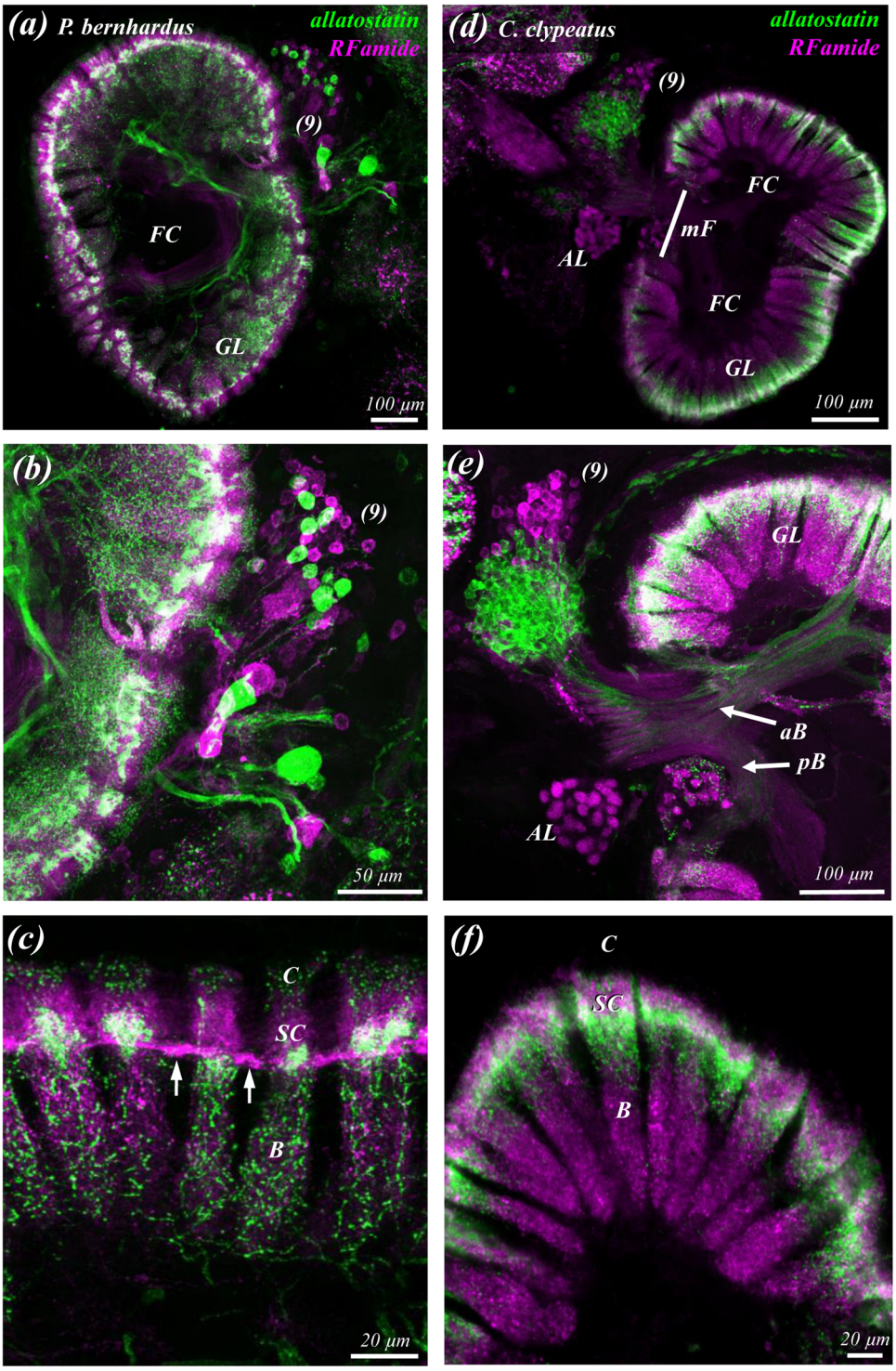

FIGURE 6 Allatostatin-like immunoreactivity (green) and RFamide-like immunoreactivity (magenta) in horizontal sections of the olfactory deutocerebrum of *P. bernhardus* (a–c, left column, showing the left olfactory lobe) and *C. clypeatus* (d–f, right column, showing the right olfactory lobe). Anterior is toward the top. For explanation of arrows, see related text. Abbreviations: aB, anterior bundle; AL, accessory lobe B, base; C, cap; GL, glomerular layer; FC, fibrous core; mF, median foramen; pB, posterior bundle; Sc, subcap; (9), (11) cell clusters (9) and (11)

sizes (Figure 9f–i). We could not trace any labeled fibers connecting the regularly spaced fields (Figure 9f). In several of these fields, the labeled material was concentrated in the periphery in a ring-like arrangement so that we will call these elements "ring terminals" in the following (Figure 9f,i).

3.3.2 | Coenobita clypeatus

Within cell cluster (9), somata with RF-ir versus AST-ir represent distinct populations located next to each other (Figure 6d,e; compare Polanska et al., 2012). Their neurites take a similar course and enter the

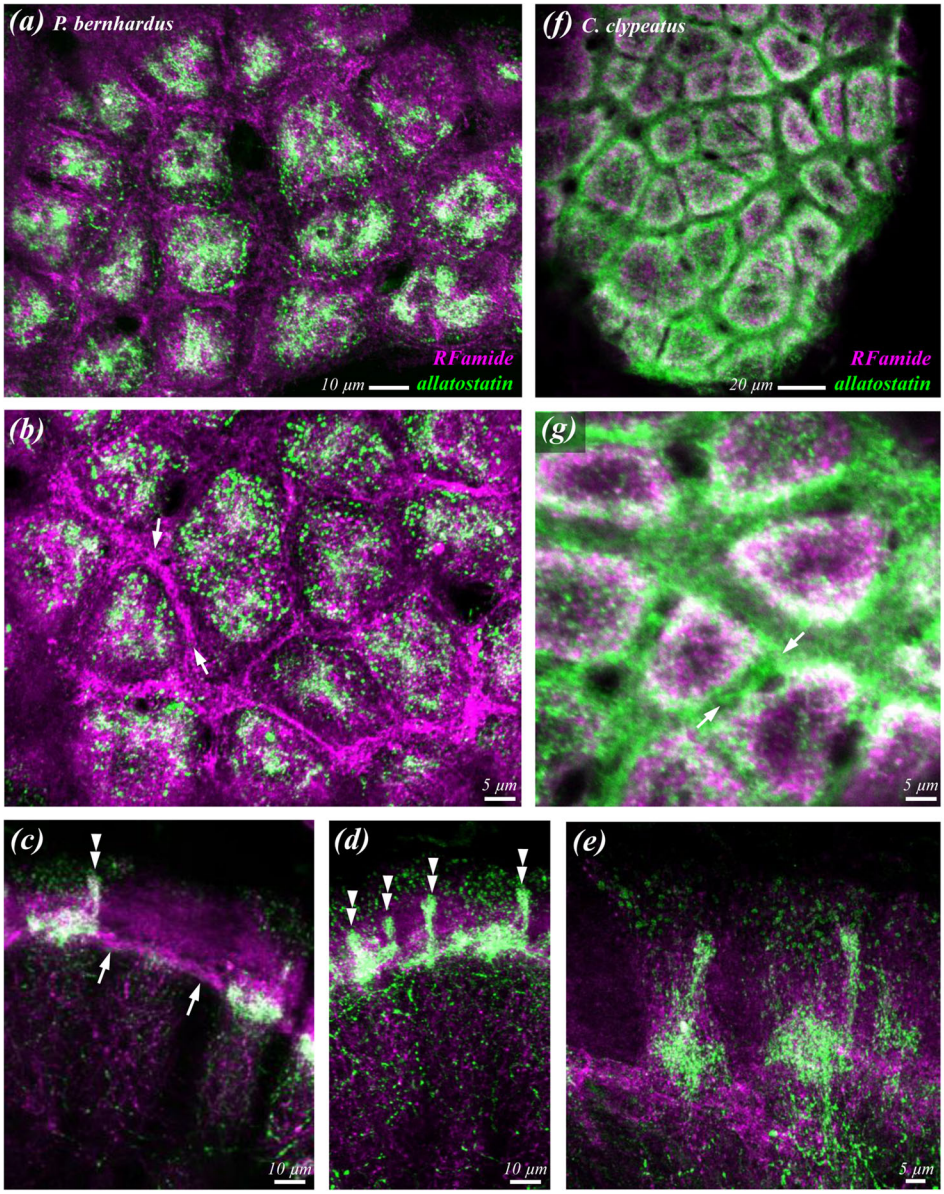

FIGURE 7 Allatostatin-like immunoreactivity (green) and RFamide-like immunoreactivity (magenta) in the olfactory glomeruli of *P. bernhardus* (a–e) and *C. clypeatus* (f–g). (c–e) Longitudinal sections of the glomeruli, and (a and b) and (f and g) transverse sections of the subcap area. For explanation of arrows and arrowheads, see related text

lobe via the mF and then split up in the anterior and posterior bundles (Figures 6e and 8c,d). Neurites with RF-ir innervate the nonglomerular neuropils c, d, and f (Figure 8c; terminology according to Harzsch & Hansson, 2008). The spherical glomeruli of the accessory lobe (AL) also show RF-ir (Figures 6d,e and 8c). Bundles of neurites with AST-ir (asterisks in Figure 8e) extend from the core of the lobe distally across the glomerular layer. There, the neurites change course to form a tangential fiber belt (paired arrows in Figure 8e), which laterally connects multiple glomeruli at the subcap level (compare Polanska et al., 2020). Tangential sections of the lobe also reveal this AST-ir immunoreactive material in the interglomerular space (arrows in Figure 7g). Higher magnification of the glomerular layer in longitudinal view shows that RF-ir is evenly distributed across the subcap and base regions of the glomeruli, and in the base a stronger signal of RF-ir is present than of AST-ir (Figure 6e,f). Cross-sections of the glomeruli show strong AST-ir in an outer ring representing the upper part of the previously described beaker domains, where an overlap with RF-ir is visible suggesting a close convergence of these two populations of neurites (Figure 7f,g).

3.4 | Marker set 4: Allatostatin-like immunoreactivity (AST-ir) and orcokinin-immunoreactivity (OK-ir)

3.4.1 | Pagurus bernhardus

Local olfactory interneurons with orcokinin-immunoreactivity (OK-ir) in cluster (9) send bundles of neurites into the olfactory lobe, some

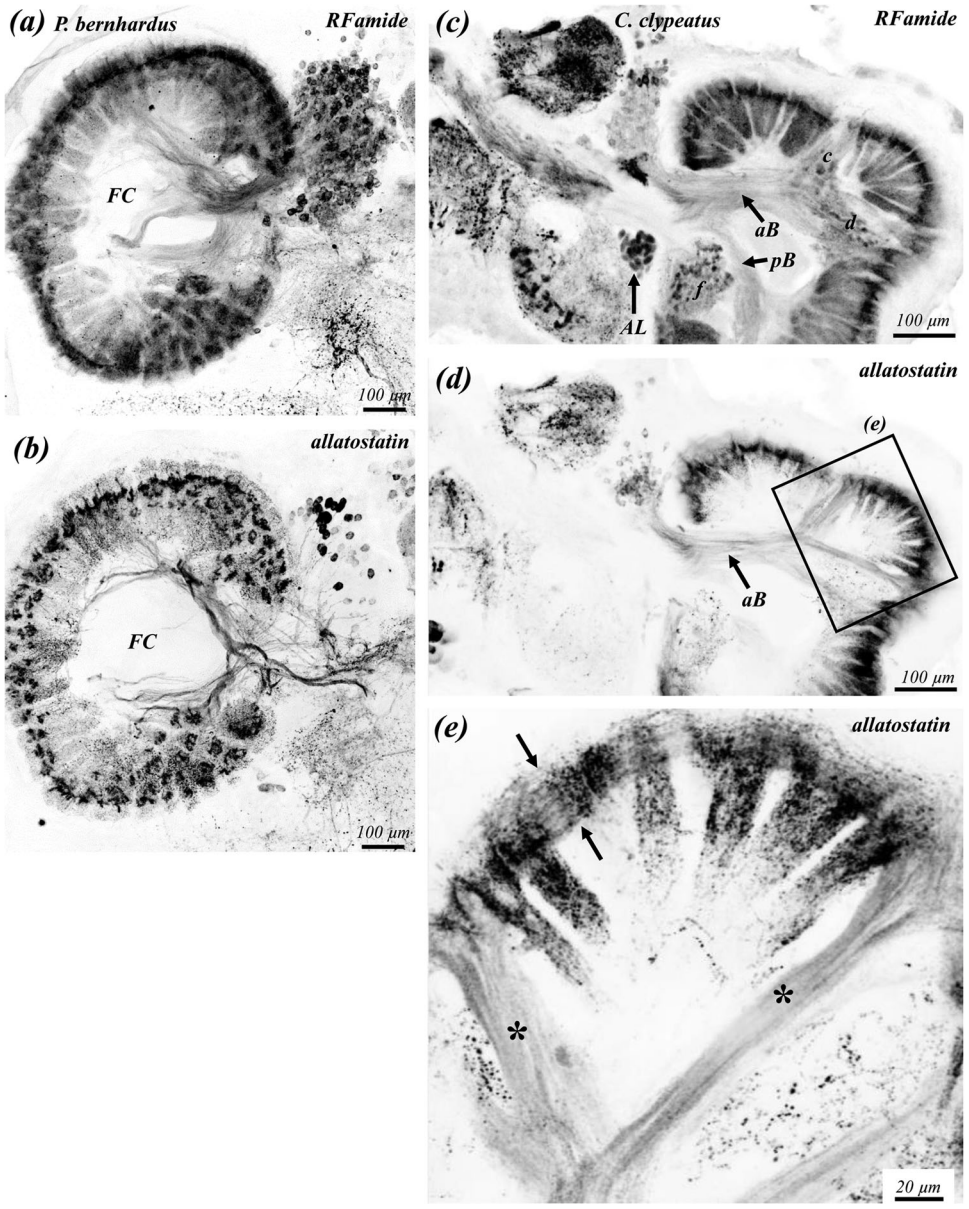

FIGURE 8 Allatostatin-like immunoreactivity and RFamide-like immunoreactivity (all images were black-white inverted) in horizontal sections of the olfactory deutocerebrum of *P. bernhardus* (a–b, left column, showing the left olfactory lobe) and *C. clypeatus* (d–f, right column, showing the right olfactory lobe; (e) modified from Polanska et al., 2020). Anterior is toward the top. For explanation of arrows and asterisks, see related text. Abbreviations: aB, anterior bundle; AL, accessory lobe; c, nonglomerular neuropil c; d, non-glomerular neuropil d; FC, fibrous core; mF, median foramen; pB, posterior bundle

of which extend across the glomerular layer to its distal part (Figure 10a,b). Others enter the base of the glomeruli (arrow in Figure 11b; see also Figure 12). All glomeruli show distinct OK-ir across their entire volume and the signal is strongest in the cap region (Figures 10c and 11b) as is also visible in the cross-sections of the glomerular layer at the cap level (Figure 11d). The previously described ring terminals with AST-ir are embedded within the OK-ir material of the cap region (inset Figure 11a). Higher magnifications of the distal part of the glomerular layer in which the orcokinin signal was amplified showed fuzzy bundles of neurites in a distal layer (dL) surrounding the lobe, some of which can be seen to extend into the cap region of the glomeruli (Figure 11a–c).

3.4.2 | Coenobita clypeatus

In accordance with our previous study (Polanska et al., 2020), all glomeruli in the lobe display strong immunoreactivity against orcokinin (Figure 10d). Within the glomeruli, the signal of OK-ir is strongest in the cap region (Figures 10f and 11e) as is also apparent in cross-sections (Figure 11h). Within cluster (9), somata with OK-ir and AST-ir are mixed, the former being larger than the latter ones (Figures 10e and 11g). The primary neurites that emerge from individual somata with OK-ir show a beaded appearance as they pass through the array of other somata in the cluster (Figures 10d and 11f,g). The swellings of

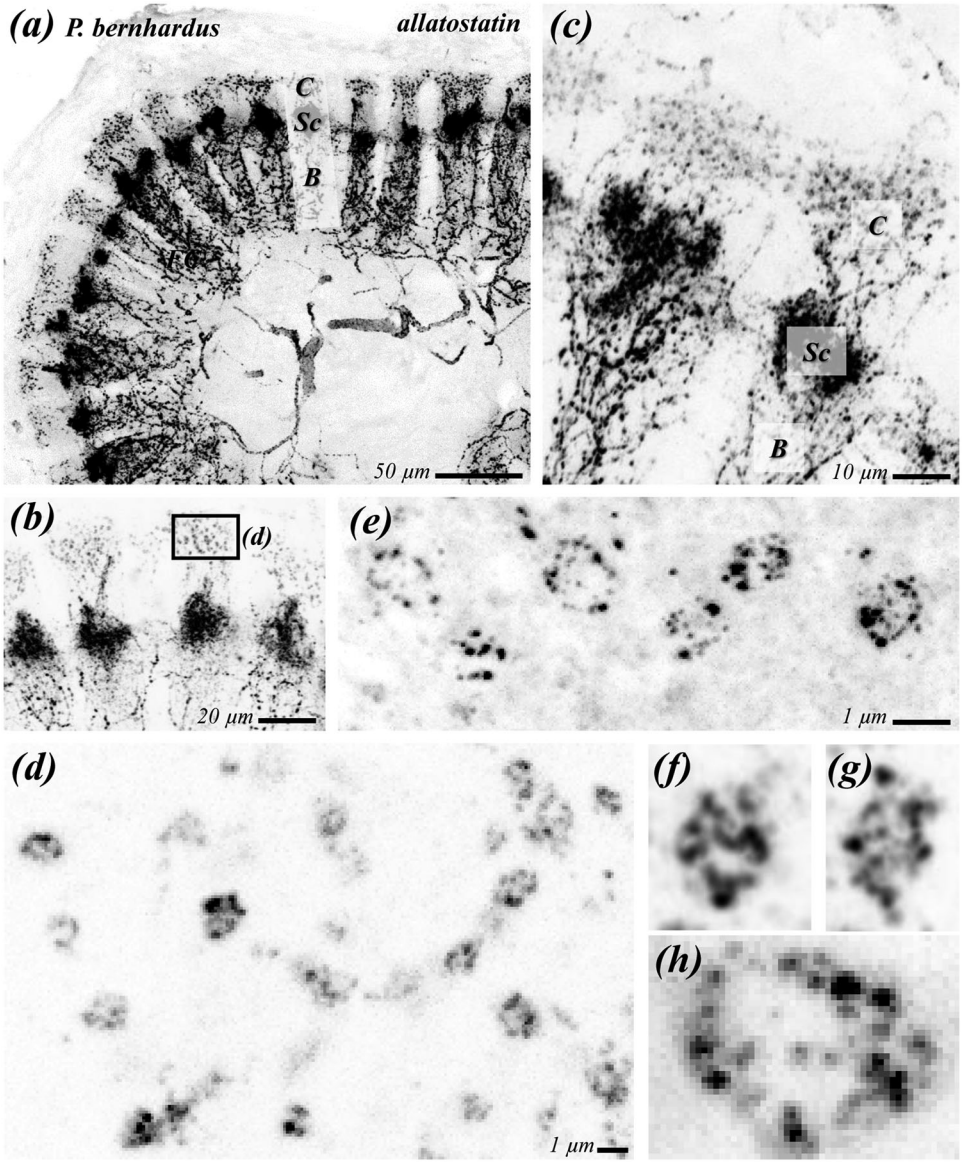

FIGURE 9 Allatostatin-like immunoreactivity (black; all images black-white inverted) in the olfactory glomeruli (longitudinal sections) of *P. bernhardus*. (e–h) Higher magnifications of the ring terminals shown in (d). For further explanation, see related text. Abbreviations: B, base; C, cap; Sc, subcap

the neurites are located in immediate vicinity to the somata with RF-ir (Figure 10g). A bundle of neurites of OK-ir neurons in cluster (9) enters the lobe to split up in the anterior and posterior bundles (Figure 10d). Polanska et al. (2020) reported that immunolabeled fibers from these bundles do not directly target the olfactory glomeruli from their proximal side, but that from nonglomerular neuropils, immunolabeled fibrous material extends laterally into the glomerular array to link neighboring glomeruli suggesting that the orcokinin-immunoreactive neurons belong to the "rim"-type of local olfactory interneurons (compare Figure 12). The antenna 1 nerve, which carries the afferent axons of olfactory sensory neurons from the first antenna, shows OK-ir (Figure 11e; compare Polanska et al., 2020). As the nerve approaches the olfactory lobe, fibers within the nerve fan out laterally over the surface of the lobe. Inside the glomeruli, labeling is strongest in the distal quarter, presumably because the signal from the afferents overlaps here with that of the interneurons.

4 | DISCUSSION

Our study reveals a yet unknown level of structural complexity of crustacean olfactory glomeruli. Furthermore, we find that despite shared features such as the compartmentalization in cap, subcap, and base regions, the glomeruli display distinct, species-specific differences with regard to the innervation pattern by the types of local olfactory interneurons that we analyzed (Figure 12). We studied one marine (*P. bernhardus*) and one terrestrial (*C. clypeatus*) hermit crab species, two groups which are nevertheless phylogenetically closely related. These

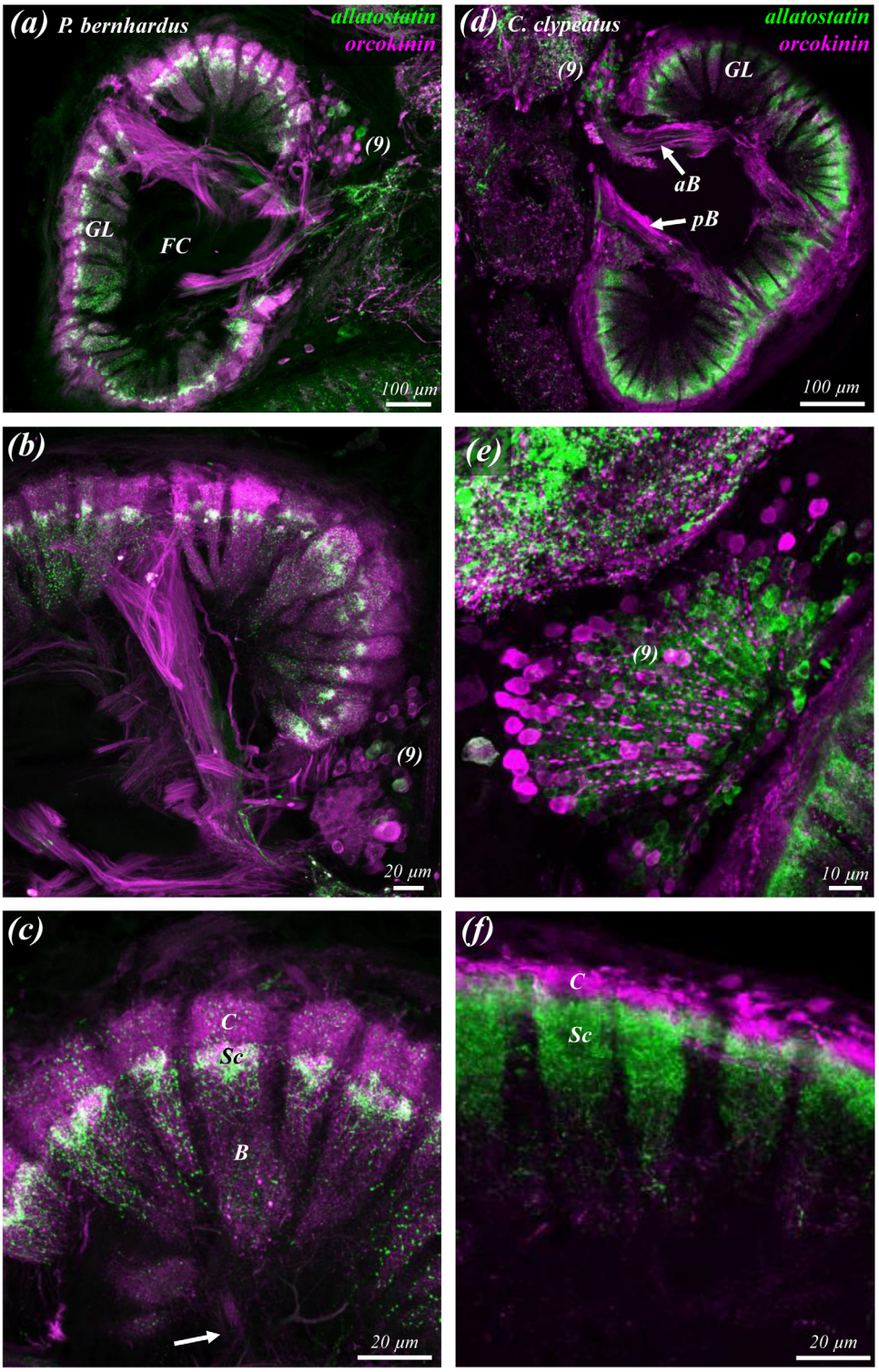

FIGURE 10 Allatostatin-like immunoreactivity (green) and orcokinin-immunoreactivity (magenta) in horizontal sections of the olfactory deutocerebrum of *P. bernhardus* (a–c, left column, showing the left olfactory lobe) and *C. clypeatus* (d–f, right column, showing the right olfactory lobe). Anterior is toward the top. For explanation of arrow, see related text. Abbreviations; aB, anterior bundle; B, base; C, cap; GL, glomerular layer; FC, fibrous core; pB, posterior bundle; Sc, subcap; (9) cell cluster (9)

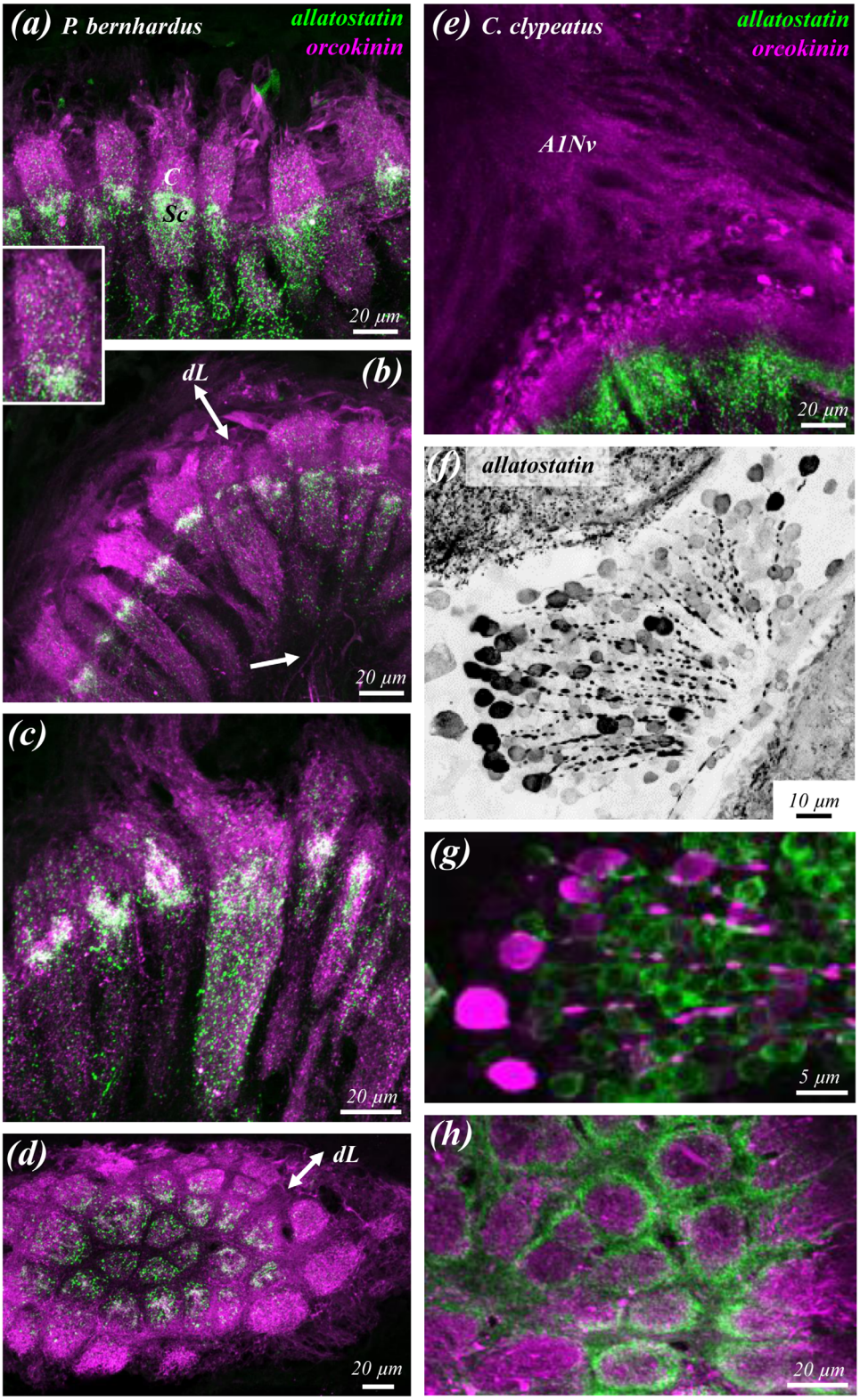

FIGURE 11 Allatostatin-like immunoreactivity (green) and orcokinin-immunoreactivity (magenta, black) in the glomeruli of *P. bernhardus* (a–d) and *C. clypeatus* (e–h). (a–c) and (e) longitudinal sections of the glomeruli, and (d and h) tangential sections of the glomerular layer. (f and g) Higher magnifications of cluster (9). For explanation of arrow, see related text. Abbreviations: A1Nv, antenna 1 nerve; B, base; C, cap; dL, distal layer; Sc, subcap

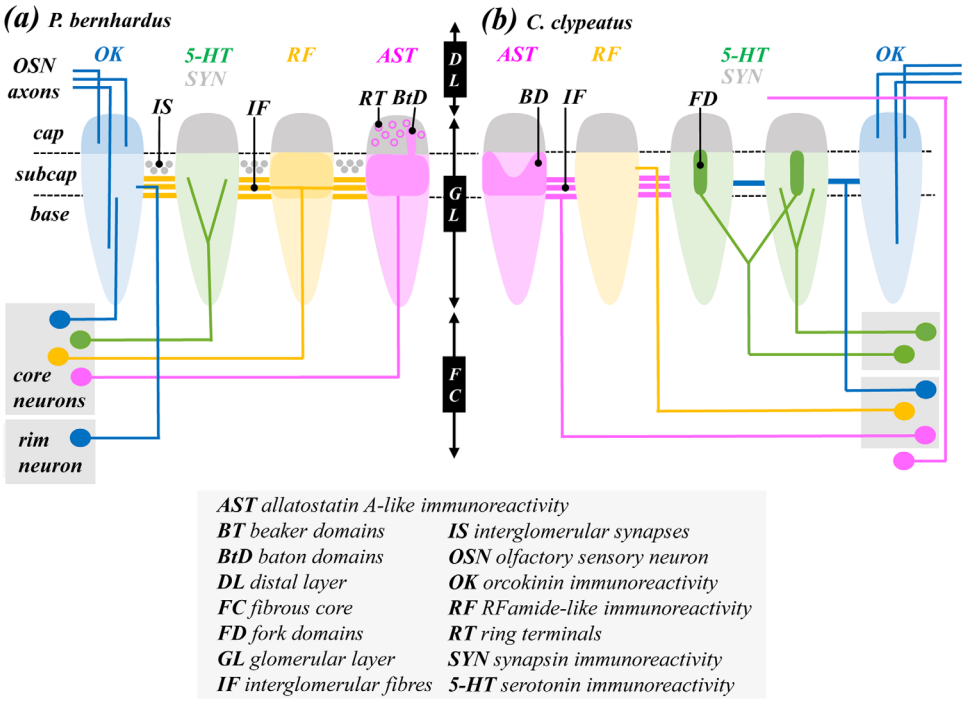

FIGURE 12 Glomerular structure and neurochemistry in *P. bernhardus* and *C. clypeatus* compiled from our previous studies (Harzsch & Hansson, 2008; Krieger et al., 2012; Polanska et al., 2012, 2020; Tuchina et al., 2015) and the present data

animals have a different olfactory physiology because it is well known that olfaction in water *versus* in air poses different demands on the process of signal reception and transduction in crustaceans so that perireceptor events may play important roles (Hansson et al., 2011; Krieger et al., 2021). Addressing the question whether different life styles acted as evolutionary drivers for functional adaptations of elements in the central olfactory pathway demands analyses with a broader taxon sampling including both additional marine and terrestrial representatives of the Anomala. We will focus the following discussion on comparing the current results to previous data obtained from representatives of the decapod crustaceans such as crayfish, clawed lobsters and spiny lobsters in which the neurochemistry of local olfactory interneurons has been analyzed in considerable depth (Table 1).

4.1 | Modulation of glomerular input

In decapod crustaceans, the axons of the olfactory sensory neurons (OSNs) associated with the aesthetascs on the first pair of antennae (Derby et al., 2016; Hallberg & Skog, 2011; Schmidt & Mellon, 2011) form a plexus-like distal layer around the periphery of the olfactory lobe. This distal layer of the lobe functions as a sorting zone in which the axons get distributed to their target glomeruli, the cap region of which they enter vertically (Beltz et al., 2003; Blaustein et al., 1988; Mellon & Alones, 1993; Sandeman & Luff, 1973; Schmidt & Ache, 1992; Tuchina et al., 2015). This compartment represents the major input region in which the afferences branch extensively (Schmidt & Ache, 1992). Acetylcholine represents the main OSN transmitter (Schachtner et al., 2005). Recently, however, orcokinin-like neuropeptides have been suggested to function as a cotransmitter in olfactory transmission (Polanska et al., 2020), a claim corroborated by the present study (Figure 12). The afferent fibers from a given cluster of OSNs associated with one aesthetasc sensillum in crayfish were shown to target many glomeruli of the lobe (Mellon & Munger, 1990; Sandeman & Denburg, 1976), and evidence obtained in spiny lobsters (Schmidt & Ache, 1992) and terrestrial hermit crabs (Tuchina et al., 2015) from antennal backfills and silver impregnation techniques indicate that both uniglomerular and multiglomerular terminations of the afferents occur frequently. These findings collectively indicate that the OSN projection pattern is nontopographic in decapod crustaceans (Mellon & Alones, 1993).

In the cap region of *P. bernhardus*, we localized AST-ir terminal profiles, the labeled material of which was concentrated in a ring-like arrangement (ring terminals) of ca. 1 μm diameter. These terminals are in a perfect position to directly modulate the OSN input (Figure 12). However, we did not record any anti-synapsin immunoreactivity in these structures, proteins associated with presynaptic vesicles that play essential roles in controlling synaptic transmission. Therefore, the ring terminals may not represent classical synapses but another novel type of release sites for the AST-neuropeptides. In the mushroom bodies of the marine chelicerate *Limulus polyphemus* (Xiphosura), afferent neurites form synaptic specializations called "ring terminals," which are 10 μm in diameter and display a similar appearance (Fahrenbach, 1979). Likewise, in the calyces of insects, microglomeruli are present in which the axons of projection neurons and Kenyon cell dendrites also form complex, ring-shaped synapses (Groh & Rössler, 2020; F. Li et al., 2020; Puñal et al., 2021; Rybak, 2013). However, these microglomeruli

display synapsin-immunoreactivity (Fahrbach & Van Nest, 2016), contrary to the ring terminals encountered in our present study. To our knowledge, ring terminals have not yet been reported from the olfactory glomeruli of any other crustacean or insect (Rybak et al., 2016; Rybak & Hansson, 2018).

4.2 | Crustacean glomeruli are regionalized into longitudinal and concentric compartments

Contrary to *P. bernhardus* in which the glomeruli display a loose network of 5HT-ir neurites similar to the situation, for example, in crayfish (references see Table 1), in *C. clypeatus* we found conspicuous rod-shaped areas of dense 5HT-ir material (rod domains) within the center of the subcap of each glomerulus. Such domains of 5HT-ir structures have not been reported previously for any other crustacean. An analysis of 5HT-ir neurons in four different decapod crustaceans revealed considerable variation in the innervation pattern of the olfactory lobe (Johansson, 1991). Although larger or giant 5HT-ir somata of olfactory interneurons project axons to terminals and fibers throughout the glomeruli (*M. rosenbergii*) or the base only (crayfish *Pacifastacus leniusculus*), smaller interneurons in the anomuran *Munida sarsi* preferentially innervate the cap region but apparently without forming rod domains (Johansson, 1991).

Nevertheless, in the spiny lobster *Panulirus argus*, similar rod- or cone-like accumulations containing Substance P-like immunoreactive neuropeptides are also located in the center of the glomerular subcap region (Schmidt & Ache, 1997; and see also Schachtner et al., 2005, their Figure 3c). In *P. argus*, the rod domains are surrounded by concentric accumulations of RF-ir terminal structures. Such a concentric arrangement is also present in *C. clypeatus* in which AST-ir structures ("beaker domains") surrounds the central 5RT-ir rod domains, whereas RF-ir neurites are evenly scattered across the glomeruli. It would appear that similar architectural features characterize the subcap area in both species and perhaps others, but curiously these are realized by interneurons with a different neurochemistry (Figure 12). In many glomeruli of *C. clypeatus*, two of the rod-shaped profiles in neighboring glomeruli stem from a single bundle of 5HT-ir neurites, and these "fork domains" anatomically link pairs of glomeruli suggesting some kind of functional cooperation of glomerular pairs.

In *P. bernhardus*, but not *C. clypeatus*, rod-shaped extensions of AST-ir structures ("baton domains") protrude from the subcap into the cap region, but these protrusions are not located in the center of the glomeruli as are the rod-domains of *C. clypeatus* (Figure 12). Comparable elements were observed in *P. argus* applying immunohistochemistry against small cardioactive peptide B. This technique revealed ball-like spots of heavily labeled material at the lateral edges of the glomeruli in the cap region (Schmidt & Ache, 1997). The glomerular cap region primarily represents an input compartment (axons of OSNs), whereas in the base, neurites of the projection neurons (PNs) assemble as output channel of the system (Harzsch & Krieger, 2018; Schachtner et al., 2005). The current findings collectively suggest that in both species studied here, the subcap region, in addition to providing lateral (most likely inhibitory) interglomerular connections (Polanska et al., 2020; Wachowiak & Ache, 1997) (and see below), may take a central computational role in modulating the information transfer from OSNs to PNs. Electron microscopic studies will shed light on the question if the central rod domains and other accumulations of strongly immunostained material in the subcap contain specialized synaptic arrangements, which may be essential for this modulatory function. Such functions are known from electron microscopic investigation of 5HT-ir and dense-cored vesicles-containing neuropeptidergic terminals (containing, e.g., pentapeptide proctolin) in crayfish central body neuropils (Schürmann et al., 1991).

4.3 | Interglomerular links

In insects, one essential step for translating the OSN input into an odor-specific, combinatorial code of glomerular activity was suggested to be a comparison across all sensory neurons in which their global activity is measured and then modulated accordingly (Galizia, 2014; Martin et al., 2011; Szyszka & Galizia, 2015; Wilson, 2013). This task may be accomplished by a network of lateral inhibitory local olfactory interneurons that branch across the glomeruli. In insects, this inhibitory network is proposed to function as a gain control in which at high odor concentrations, activity surrounding specific glomeruli is suppressed and interglomerular contrast is enhanced (Galizia, 2014; Szyszka & Galizia, 2015). In spiny lobsters, many local interneurons innervate large ensembles of glomeruli, in some cases up to 85% of the entire glomerular array (Wachowiak et al., 1997). In these crustaceans, certain types of "rim" interneurons, some of which are inhibitory GABAergic or histaminergic (Wachowiak et al., 1997; Wachowiak & Ache, 1997; Wachowiak & Cohen, 1999), have been suggested to provide massive lateral inhibitory connections across the glomerular ensemble (Schmidt & Ache, 1996; Schmidt & Mellon, 2011). In crayfish, such lateral connections earlier on were described as "interglomerular fibers" (Blaustein et al., 1988), and Polanska et al. (2020) provided evidence for massive lateral connections across the glomerular array in *C. clypeatus*. Thus, rim neurons may represent key elements mediating lateral inhibitory interactions by modulating the transfer of OSN input to the projection neurons through presynaptic afferent inhibition (Schmidt & Ache, 1996; Wachowiak et al., 1997; Wachowiak & Ache, 1997). In all decapod crustaceans investigated so far, the glomeruli are arranged in a strictly radial array, each glomerulus lying in parallel and equally spaced to its immediate neighbors. Harzsch and Krieger (2018) proposed that the subcap connections by interglomerular fibers may be the driving evolutionary force for such a geometrical layout that optimizes wiring expenses and may be beneficial for synchronizing lateral inhibition.

In *C. clypeatus*, the neurochemical diversity of "rim" interneurons that laterally connect glomeruli includes AST (Harzsch & Hansson, 2008; Polanska et al., 2012) and orcokinin (Polanska et al., 2020). In *P. bernhardus*, we found that interglomerular fibers display strong RF-ir but not any AST-ir, which is so typical for *C. clypeatus*. Yet, in *P. bernhardus*, but not *C. clypeatus*, presynaptic material was labeled in the interglomerular space between the subcap regions of

neighboring glomeruli (Figure 12). Although the neurochemistry of the pre- and postsynaptic elements could not be resolved in our study, these findings nevertheless suggest that synaptic interactions in the interglomerular space play a role in olfactory processing, adding yet another layer of complexity to our knowledge of olfactory systems in crustaceans.

5 | CONCLUSIONS AND OUTLOOK

Aspects of glomerular regionalization and neuronal diversity in the crustacean olfactory deutocerebrum have already been analyzed by immunohistochemistry more than 20 years ago (Schmidt & Ache, 1997). Here, we systematically combined immunohistochemistry with the power of confocal laser-scan microscopy to analyze the glomerular architecture revealing an unexpected level of structural complexity including interglomerular synapses. Peptidergic and aminergic interneurons provide the structural basis for a regionalization of the crustacean glomeruli into longitudinal and concentric compartments. Our data suggest that local olfactory interneurons take a central role in mediating lateral inhibitory interactions across the glomerular array and in modulating the information transfer from olfactory sensory neurons to projection neurons within the glomeruli.

Our results revealed dense areas of fine, strongly immunoreactive material in the subcap region which we termed baton, rod, and fork domains. Connectomic reconstructions at the electron microscopic level have recently provided structural insights into the brain of the fruit fly *D. melanogaster* of unprecedented detail (Scheffer et al., 2020; Zheng et al., 2018), and such data sets today embrace, for example, the mushroom body (F. Li et al., 2020), the projection neuron pathway (Bates et al., 2020), and the projection neuron-to-Kenyon cell connectivity (Zheng et al., 2020). Similar technical approaches should be well suited to analyze the central domains of the crustacean glomeruli at an ultrastructural level in search for specialized synaptic arrangements.

The amazing structural complexity of crustacean glomeruli as analyzed by light microscopy is unmatched by what is known about insect olfactory glomeruli. However, using electron microscopy, olfactory glomerular microcircuits are being intensely studied in insects, and such analyses have revealed a high complexity at the ultrastructural level including reciprocal dendrodendritic synapses, triad configurations, and polyadic synapses (e.g., Bates et al., 2020; Rybak et al., 2016). The most recent phylogenomic studies collectively suggest that crustaceans in the traditional sense are the closest relatives of hexapods or that hexapods are in fact an ingroup of Crustacea (Lozano-Fernandez et al., 2016; Misof et al., 2014; Schwentner et al., 2017; Wipfler et al., 2019). Similarities and differences between hexapod and crustacean olfactory systems concerning, for example, numbers and shape of olfactory glomeruli, connectivity from sensory neuron to glomerulus, numbers and morphology of olfactory interneurons, persistent adult neurogenesis, and projection neuron targets have highlighted the need to study crustacean brains in order to understand structure and function of insect brains (Harzsch & Krieger, 2018, 2021; Wittfoth & Harzsch, 2018). Therefore, the exploration of crustacean olfactory systems should continue, and analyses of olfactory glomerular microcircuits would be a logical next step.

ACKNOWLEDGMENTS

We wish to thank Jürgen Rybak for discussion on glomerular morphology in arthropod brains. This study was supported by DFG grant Ha 2540/19-1 and the Max Planck Society.

Open access funding enabled and organized by Projekt DEAL.

DATA AVAILABILITY STATEMENT

The data that support the findings of this study are available from the corresponding author upon reasonable request.

ORCID

Steffen Harzsch https://orcid.org/0000-0002-8645-3320

REFERENCES

Antonsen, B. L., & Paul, D. H. (2001). Serotonergic and octopaminergic systems in the squat lobster *Munida quadrispina* (anomura, galatheidae). *The Journal of Comparative Neurology*, *439*(4), 450–468. https://doi.org/10.1002/cne.1362

Bates, A. S., Schlegel, P., Roberts, R. J. V., Drummond, N., Tamimi, I. F. M., Turnbull, R., Zhao, X., Marin, E. C., Popovici, P. D., Dhawan, S., Jamasb, A., Javier, A., Serratosa Capdevila, L., Li, F., Rubin, G. M., Waddell, S., Bock, D. D., Costa, M., & Jefferis, G. S. X. E. (2020). Complete connectomic reconstruction of olfactory projection neurons in the fly brain. *Current Biology*, *30*(16), 3183–3199.e6. https://doi.org/10.1016/j.cub.2020.06.042

Beltz, B. S. (1999). Distribution and functional anatomy of amine-containing neurons in decapod crustaceans. *Microscopy Research and Technique*, *44*(2–3), 105–120. https://doi.org/10.1002/(SICI)1097-0029(19990115/01)44:2/3⟨105::AID-JEMT5⟩3.0.CO;2-K

Beltz, B. S., Kordas, K., Lee, M. M., Long, J. B., Benton, J. L., & Sandeman, D. C. (2003). Ecological, evolutionary, and functional correlates of sensilla number and glomerular density in the olfactory system of decapod crustaceans. *The Journal of Comparative Neurology*, *455*(2), 260–269.

Beltz, B. S., Pontes, M., Helluy, S. M., & Kravitz, E. A. (1990). Patterns of appearance of serotonin and proctolin immunoreactivities in the developing nervous system of the American lobster. *Journal of Neurobiology*, *21*(4), 521–542. https://doi.org/10.1002/neu.480210402

Benton, J. L., Sandeman, D. C., & Beltz, B. S. (2007). Nitric oxide in the crustacean brain: Regulation of neurogenesis and morphogenesis in the developing olfactory pathway. *Developmental Dynamics*, *236*(11), 3047–3060. https://doi.org/10.1002/dvdy.21340

Blaustein, D. N., Derby, C. D., Simmons, R. B., & Beall, A. C. (1988). Structure of the brain and medulla terminalis of the spiny lobster *Panulirus argus* and the crayfish *Procambarus clarkii*, with an emphasis on olfactory centers. *Journal of Crustacean Biology*, *8*, 493–519.

Bungart, D., Dircksen, H., & Keller, R. (1994). Quantitative determination and distribution of the myotropic neuropeptide orcokinin in the nervous system of astacidean crustaceans. *Peptides*, *15*(3), 393–400. https://doi.org/10.1016/0196-9781(94)90194-5

Bungart, D., Hilbich, C., Dircksen, H., & Keller, R. (1995). Occurrence of analogues of the myotropic neuropeptide orcokinin in the shore crab, *Carcinus maenas*: Evidence for a novel neuropeptide family. *Peptides*, *16*(1), 67–72. https://doi.org/10.1016/0196-9781(94)00145-v

Cape, S. S., Rehm, K. J., Ma, M., Marder, E., & Li, L. (2008). Mass spectral comparison of the neuropeptide complement of the stomatogastric ganglion and brain in the adult and embryonic lobster, *Homarus americanus*. *Journal of Neurochemistry*, *105*(3), 690–702. https://doi.org/10.1111/j.1471-4159.2007.05154.x

Christie, A. E. (2014). Expansion of the *Litopenaeus vannamei* and *Penaeus monodon* peptidomes using transcriptome shotgun assembly sequence

data. *General and Comparative Endocrinology*, *206*, 235–254. https://doi.org/10.1016/j.ygcen.2014.04.015

Christie, A. E. (2016). Expansion of the neuropeptidome of the globally invasive marine crab *Carcinus maenas*. *General and Comparative Endocrinology*, *235*, 150–169. https://doi.org/10.1016/j.ygcen.2016.05.013

Christie, A. E., & Chi, M. (2015). Neuropeptide discovery in the Araneae (Arthropoda, Chelicerata, Arachnida): Elucidation of true spider peptidomes using that of the Western black widow as a reference. *General and Comparative Endocrinology*, *213*, 90–109. https://doi.org/10.1016/j.ygcen.2015.02.003

Christie, A. E., Sousa, G. L., Rus, S., Smith, C. M., Towle, D. W., Hartline, D. K., & Dickinson, P. S. (2008). Identification of A-type allatostatins possessing −YXFGI/Vamide carboxy-termini from the nervous system of the copepod crustacean *Calanus finmarchicus*. *General and Comparative Endocrinology*, *155*(3), 526–533. https://doi.org/10.1016/j.ygcen.2007.09.002

Christie, A. E., Stemmler, E. A., & Dickinson, P. S. (2010). Crustacean neuropeptides. *Cellular and Molecular Life Sciences: CMLS*, *67*(24), 4135–4169. https://doi.org/10.1007/s00018-010-0482-8

Derby, C. D., Kozma, M. T., Senatore, A., & Schmidt, M. (2016). Molecular mechanisms of reception and perireception in crustacean chemoreception: A comparative review. *Chemical Senses*, 1–18. https://doi.org/10.1093/chemse/bjw057

Derby, C. D., & Weissburg, M. J. (2014). The chemical senses and chemosensory ecology of crustaceans. In C. D. Derby & M. Thiel (Eds.), *Crustacean nervous systems and their control of behavior* (pp. 263–292). Oxford University Press.

Dircksen, H., Burdzik, S., Sauter, A., & Keller, R. (2000). Two orcokinins and the novel octapeptide orcomyotropin in the hindgut of the crayfish *Orconectes limosus*: Identified myostimulatory neuropeptides originating together in neurones of the terminal abdominal ganglion. *The Journal of Experimental Biology*, *203*(Pt 18), 2807–2818.

Dircksen, H., Neupert, S., Predel, R., Verleyen, P., Huybrechts, J., Strauss, J., Hauser, F., Stafflinger, E., Schneider, M., Pauwels, K., Schoofs, L., & Grimmelikhuijzen, C. J. P. (2011). Genomics, transcriptomics, and peptidomics of *Daphnia pulex* Neuropeptides and protein hormones. *Journal of Proteome Research*, *10*(10), 4478–4504. https://doi.org/10.1021/pr200284e

Dircksen, H., Skiebe, P., Abel, B., Agricola, H., Buchner, K., Muren, J. E., & Nässel, D. R. (1999). Structure, distribution, and biological activity of novel members of the allatostatin family in the crayfish *Orconectes limosus*. *Peptides*, *20*(6), 695–712. https://doi.org/10.1016/s0196-9781(99)00052-2

Dockray, G. (2004). The expanding family of -RFamide peptides and their effects on feeding behaviour. *Experimental Physiology*, *89*(3), 229–235. https://doi.org/10.1113/expphysiol.2004.027169

Duve, H., Johnsen, A. H., Scott, A. G., & Thorpe, A. (2002). Allatostatins of the tiger prawn, *Penaeus monodon* (Crustacea: Penaeidea). *Peptides*, *23*(6), 1039–1051. https://doi.org/10.1016/s0196-9781(02)00035-9

Fahrbach, S. E., & Van Nest, B. N. (2016). Synapsin-based approaches to brain plasticity in adult social insects. *Current Opinion in Insect Science*, *18*, 27–34. https://doi.org/10.1016/j.cois.2016.08.009

Fahrenbach, W. (1979). The brain of the horseshoe crab (*Limulus polyphemus*). III. Cellular and synaptic organization of the corpora pedunculata. *Tissue & Cell*, *11*, 163–199. https://doi.org/10.1016/0040-8166(79)90016-8

Fuscà, D., & Kloppenburg, P. (2021). Odor processing in the cockroach antennal lobe—The network components. *Cell and Tissue Research*, *383*(1), 59–73. https://doi.org/10.1007/s00441-020-03387-3

Galizia, C. G. (2014). Olfactory coding in the insect brain: Data and conjectures. *European Journal of Neuroscience*, *39*(11), 1784–1795. https://doi.org/10.1111/ejn.12558

Galizia, C. G., & Rössler, W. (2010). Parallel olfactory systems in insects: Anatomy and function. *Annual Review of Entomology*, *55*(1), 399–420. https://doi.org/10.1146/annurev-ento-112408-085442

Groh, C., & Rössler, W. (2020). Analysis of synaptic microcircuits in the mushroom bodies of the honeybee. *Insects*, *11*(1), 43. https://doi.org/10.3390/insects11010043

Hallberg, E., & Skog, M. (2011). Chemosensory sensilla in crustaceans. In T. Breithaupt & M. Thiel, (Eds.), *Chemical communication in crustaceans* (pp. 103–21). Springer.

Hansson, B. S., & Anton, S. (2000). Function and morphology of the antennal lobe: New developments. *Annual Review of Entomology*, *45*(1), 203–231.

Hansson, B. S., Harzsch, S., Knaden, M., & Stensmyr, M. C. (2011). The neural and behavioral basis of chemical communication in terrestrial crustaceans. In T. Breithaupt & M. Thiel (Eds.), *Chemical communication in crustaceans* (pp. 149–173). Springer.

Harzsch, S. (2002). The phylogenetic significance of crustacean optic neuropils and chiasmata: A re-examination. *The Journal of Comparative Neurology*, *453*(1), 10–21. https://doi.org/10.1002/cne.10375

Harzsch, S., & Hansson, B. S. (2008). Brain architecture in the terrestrial hermit crab *Coenobita clypeatus* (Anomura, Coenobitidae), a crustacean with a good aerial sense of smell. *BMC Neuroscience*, *9*(1), 58. https://doi.org/10.1186/1471-2202-9-58

Harzsch, S., & Krieger, J. (2018). Crustacean olfactory systems: A comparative review and a crustacean perspective on insect olfactory systems. *Progress in Neurobiology*, *161*, 23–60.

Harzsch, S., & Krieger, J. (2021). Genealogical relationships of mushroom bodies, hemiellipsoid bodies, and their afferent pathways in the brains of Pancrustacea: Recent progress and open questions. *Arthropod Structure and Development*, *65*, 101100.

Harzsch, S., Miller, J., Benton, J. L., & Beltz, B. S. (1999). From embryo to adult: Persistent neurogenesis and apoptotic cell death shape the lobster deutocerebrum. *The Journal of Neuroscience*, *19*(9), 3472–3485.

Harzsch, S., Miller, J., Benton, J. L., Dawirs, R. R., & Beltz, B. S. (1998). Neurogenesis in the thoracic neuromeres of two crustaceans with different types of metamorphic development. *The Journal of Experimental Biology*, *201*(17), 2465–2479.

Helluy, S., Sandeman, R. E., Beltz, B. S., & Sandeman, D. C. (1993). Comparative brain ontogeny of the crayfish and clawed lobster: Implications of direct and larval development. *The Journal of Comparative Neurology*, *335*(3), 343–354. https://doi.org/10.1002/cne.903350305

Hofer, S., Dircksen, H., Tollbäck, P., & Homberg, U. (2005). Novel insect orcokinins: Characterization and neuronal distribution in the brains of selected dicondylian insects. *The Journal of Comparative Neurology*, *490*(1), 57–71. https://doi.org/10.1002/cne.20650

Hofer, S., & Homberg, U. (2006a). Evidence for a role of orcokinin-related peptides in the circadian clock controlling locomotor activity of the cockroach *Leucophaea maderae*. *The Journal of Experimental Biology*, *209*(Pt 14), 2794–2803. https://doi.org/10.1242/jeb.02307

Hofer, S., & Homberg, U. (2006b). Orcokinin immunoreactivity in the accessory medulla of the cockroach *Leucophaea maderae*. *Cell and Tissue Research*, *325*(3), 589–600. https://doi.org/10.1007/s00441-006-0155-y

Huybrechts, J., Nusbaum, M. P., Bosch, L. V., Baggerman, G., De Loof, A., & Schoofs, L. (2003). Neuropeptidomic analysis of the brain and thoracic ganglion from the Jonah crab. *Cancer borealis*. *Biochemical and Biophysical Research Communications*, *308*(3), 535–544. https://doi.org/10.1016/s0006-291x(03)01426-8

Imai, T. (2014). Construction of functional neuronal circuitry in the olfactory bulb. *Seminars in Cell & Developmental Biology*, *35*, 180–188. https://doi.org/10.1016/j.semcdb.2014.07.012

Johansson, K. U. I. (1991). Identification of different types of serotonin-like immunoreactive olfactory interneurons in four infraorders of decapod crustaceans. *Cell and Tissue Research*, *264*(2), 357–362. https://doi.org/10.1007/BF00313974

Johansson, K. U. I., Lundquist, C. T., Hallberg, E., & Nässel, D. R. (1999). Tachykinin-related neuropeptide in the crayfish olfactory midbrain.

Cell and Tissue Research, *296*(2), 405–415. https://doi.org/10.1007/s004410051300

Johansson, K. U. I., & Mellon, D. (1998). Nitric oxide as a putative messenger molecule in the crayfish olfactory midbrain. *Brain Research*, *807*(1), 237–242. https://doi.org/10.1016/S0006-8993(98)00826-9

Klagges, B. R., Heimbeck, G., Godenschwege, T. A., Hofbauer, A., Pflugfelder, G. O., Reifegerste, R., Reisch, D., Schaupp, M., Buchner, S., & Buchner, E. (1996). Invertebrate synapsins: A single gene codes for several isoforms in *Drosophila*. *The Journal of Neuroscience*, *16*(10), 3154–3165.

Kobierski, L. A., Beltz, B. S., Trimmer, B. A., & Kravitz, E. A. (1987). FMRFamidelike peptides of homarus americanus: Distribution, immunocytochemical mapping, and ultrastructural localization in terminal varicosities. *The Journal of Comparative Neurology*, *266*(1), 1–15. https://doi.org/10.1002/cne.902660102

Kotsyuba, E., & Dyachuk, V. (2021). Localization of neurons expressing choline acetyltransferase, serotonin and/or FMRFamide in the central nervous system of the decapod shore crab *Hemigrapsus sanguineus*. *Cell and Tissue Research*, *383*(3), 959–977. https://doi.org/10.1007/s00441-020-03309-3

Kotsyuba, E., Dyuizen, I., & Lamash, N. (2010). Stress-induced changes in the nitric oxide system of shore crabs living under different ecological conditions. *Russian Journal of Marine Biology*, *36*, 201–208. https://doi.org/10.1134/S1063074010030065

Kotsyuba, E. P. (2012). Distribution of neurons containing catecholamines in brain of hermit crab *Pagurus middendorffii* and of king crab *Paralithodes camtschaticus* (Anomura, Decapoda). *Cell and Tissue Biology*, *6*(4), 376–382. https://doi.org/10.1134/S1990519x12040074

Kreissl, S., Strasser, C., & Galizia, C. G. (2010). Allatostatin immunoreactivity in the honeybee brain. *The Journal of Comparative Neurology*, *518*(9), 1391–1417. https://doi.org/10.1002/cne.22343

Kress, T., Harzsch, S., & Dircksen, H. (2016). Neuroanatomy of the optic ganglia and central brain of the water flea *Daphnia magna* (Crustacea, Cladocera). *Cell and Tissue Research*, *363*(3), 649–677. https://doi.org/10.1007/s00441-015-2279-4

Krieger, J., Braun, P., Rivera, N. T., Schubart, C. D., Müller, C. H. G., & Harzsch, S. (2015). Comparative analyses of olfactory systems in terrestrial crabs (Brachyura): Evidence for aerial olfaction? *PeerJ*, *3*, e1433. https://doi.org/10.7717/peerj.1433

Krieger, J., Hörnig, M. K., Kenning, M., Hansson, B. S., & Harzsch, S. (2021). More than one way to smell ashore—Evolution of the olfactory pathway in terrestrial malacostracan crustaceans. *Arthropod Structure and Development*.

Krieger, J., Sandeman, R. E., Sandeman, D. C., Hansson, B. S., & Harzsch, S. (2010). Brain architecture of the largest living land arthropod, the giant robber crab *Birgus latro* (Crustacea, Anomura, Coenobitidae): Evidence for a prominent central olfactory pathway? *Frontiers in Zoology*, *7*(1), 1–31.

Krieger, J., Sombke, A., Seefluth, F., Kenning, M., Hansson, B. S., & Harzsch, S. (2012). Comparative brain architecture of the European shore crab *Carcinus maenas* (Brachyura) and the common hermit crab *Pagurus bernhardus* (Anomura) with notes on other marine hermit crabs. *Cell and Tissue Research*, *348*(1), 47–69. https://doi.org/10.1007/s00441-012-1353-4

Ladislav, R., Ladislav, Š., Akira, M., Mirko, S., Yoonseong, P., & Dušan, Ž. (2015). Orcokinin-like immunoreactivity in central neurons innervating the salivary glands and hindgut of ixodid ticks. *Cell and Tissue Research*, *360*(2), 209–222. https://doi.org/10.1007/s00441-015-2121-z

Langworthy, K., Helluy, S., Benton, J., & Beltz, B. (1997). Amines and peptides in the brain of the American lobster: Immunocytochemical localization patterns and implications for brain function. *Cell and Tissue Research*, *288*(1), 191–206. https://doi.org/10.1007/s004410050806

Li, F., Lindsey, J. W., Marin, E. C., Otto, N., Dreher, M., Dempsey, G., Stark, I., Bates, A. S., Pleijzier, M. W., Schlegel, P., Nern, A., Takemura, S., Eckstein, N., Yang, T., Francis, A., Braun, A., Parekh, R., Costa, M., Scheffer, L. K., … Rubin, G. M. (2020). The connectome of the adult *Drosophila* mushroom body provides insights into function. *eLife*, *9*, e62576. https://doi.org/10.7554/eLife.62576

Li, L., Pulver, S. R., Kelley, W. P., Thirumalai, V., Sweedler, J. V., & Marder, E. (2002). Orcokinin peptides in developing and adult crustacean stomatogastric nervous systems and pericardial organs. *The Journal of Comparative Neurology*, *444*(3), 227–244. https://doi.org/10.1002/cne.10139

Lozano-Fernandez, J., Carton, R., Tanner, A. R., Puttick, M. N., Blaxter, M., Vinther, J., Olesen, J., Giribet, G., Edgecombe, G. D., & Pisani, D. (2016). A molecular palaeobiological exploration of arthropod terrestrialization. *Philosophical Transactions of the Royal Society B: Biological Sciences*, *371*(1699), 20150133. https://doi.org/10.1098/rstb.2015.0133

Martin, J. P., Beyerlein, A., Dacks, A. M., Reisenman, C. E., Riffell, J. A., Lei, H., & Hildebrand, J. G. (2011). The neurobiology of insect olfaction: Sensory processing in a comparative context. *Progress in Neurobiology*, *95*(3), 427–447. https://doi.org/10.1016/j.pneurobio.2011.09.007

Maza, F. J., Sztarker, J., Shkedy, A., Peszano, V. N., Locatelli, F. F., & Delorenzi, A. (2016). Context-dependent memory traces in the crab's mushroom bodies: Functional support for a common origin of high-order memory centers. *Proceedings of the National Academy of Sciences*, *113*(49), E7957–E7965. https://doi.org/10.1073/pnas.1612418113

Mellon, D., & Alones, V. (1993). Cellular organization and growth-related plasticity of the crayfish olfactory midbrain. *Microscopy Research and Technique*, *24*(3), 231–259. https://doi.org/10.1002/jemt.1070240304

Mellon, D., & Munger, S. D. (1990). Nontopographic projection of olfactory sensory neurons in the crayfish brain. *The Journal of Comparative Neurology*, *296*(2), 253–262. https://doi.org/10.1002/cne.902960205

Mercier, A. J., Friedrich, R., & Boldt, M. (2003). Physiological functions of FMRFamide-like peptides (FLPs) in crustaceans. *Microscopy Research and Technique*, *60*(3), 313–324. https://doi.org/10.1002/jemt.10270

Misof, B., Liu, S., Meusemann, K., Peters, R. S., Donath, A., Mayer, C., Frandsen, P. B., Ware, J., Flouri, T., Beutel, R. G., Niehuis, O., Petersen, M., Izquierdo-Carrasco, F., Wappler, T., Rust, J., Aberer, A. J., Aspöck, U., Aspöck, H., Bartel, D., … Zhou, X. (2014). Phylogenomics resolves the timing and pattern of insect evolution. *Science*, *346*(6210), 763–767. https://doi.org/10.1126/science.1257570

Mombaerts, P. (2006). Axonal wiring in the mouse olfactory system. *Annual Review of Cell and Developmental Biology*, *22*(1), 713–737. https://doi.org/10.1146/annurev.cellbio.21.012804.093915

Nässel, D. R., & Homberg, U. (2006). Neuropeptides in interneurons of the insect brain. *Cell and Tissue Research*, *326*(1), 1–24. https://doi.org/10.1007/s00441-006-0210-8

Ollivaux, P. (2002). Enkephalinergic control of the secretory activity of neurons producing stereoisomers of crustacean hyperglycemic hormone in the eyestalk of the crayfish *Orconectes limosus*—Ollivaux—2002. *The Journal of Comparative Neurology*, *444*, 1–9. https://onlinelibrary.wiley.com/doi/full/10.1002/cne.1426?sid=nlm%3Apubmed

Orona, E., & Ache, B. W. (1992). Physiological and pharmacological evidence for histamine as a neurotransmitter in the olfactory CNS of the spiny lobster. *Brain Research*, *590*(1–2), 136–143. https://doi.org/10.1016/0006-8993(92)91089-W

Orona, E., Batelle, B. A., & Ache, B. W. (1990). Immunohistochemical and biochemical evidence for the putative inhibitory neurotransmitters histamine and GABA in lobster olfactory lobes. *The Journal of Comparative Neurology*, *294*(4), 633–646.

Polanska, M. A., Kirchhoff, T., Dircksen, H., Hansson, B. S., & Harzsch, S. (2020). Functional morphology of the primary olfactory centers in the brain of the hermit crab *Coenobita clypeatus* (Anomala, Coenobitidae). *Cell and Tissue Research*, *380*(3), 449–467. https://doi.org/10.1007/s00441-020-03199-5

Polanska, M. A., Tuchina, O., Agricola, H., Hansson, B. S., & Harzsch, S. (2012). Neuropeptide complexity in the crustacean central olfactory pathway: Immunolocalization of A-type allatostatins and RFamide-like peptides in the brain of a terrestrial hermit crab. *Molecular Brain*, *5*(1), 1–17. https://doi.org/10.1186/1756-6606-5-29

Puñal, V. M., Ahmed, M., Thornton-Kolbe, E. M., & Clowney, E. J. (2021). Untangling the wires: Development of sparse, distributed connectivity in the mushroom body calyx. *Cell and Tissue Research*, *383*(1), 91–112. https://doi.org/10.1007/s00441-020-03386-4

Rybak, J. (2013). Exploring brain connectivity in insect model systems of learning and memory. In *Invertebrate learning and memory* (pp. 26–40). Elsevier. http://linkinghub.elsevier.com/retrieve/pii/B9780124158238000046

Rybak, J., & Hansson, B. S. (2018). Olfactory microcircuits in *Drosophila melanogaster*. In *Handbook of brain microcircuits* (2nd ed., pp. 361–367). Oxford University Press. https://pure.mpg.de/pubman/faces/ViewItemOverviewPage.jsp?itemId=item_2565272

Rybak, J., Talarico, G., Ruiz, S., Arnold, C., Cantera, R., & Hansson, B. S. (2016). Synaptic circuitry of identified neurons in the antennal lobe of *Drosophila melanogaster*. *The Journal of Comparative Neurology*, *524*(9), 1920–1956. https://doi.org/10.1002/cne.23966

Saetan, J., Senarai, T., Tamtin, M., Weerachatyanukul, W., Chavadej, J., Hanna, P. J., Parhar, I., Sobhon, P., & Sretarugsa, P. (2013). Histological organization of the central nervous system and distribution of a gonadotropin-releasing hormone-like peptide in the blue crab, *Portunus pelagicus*. *Cell and Tissue Research*, *353*(3), 493–510. https://doi.org/10.1007/s00441-013-1650-6

Sandeman, D. C., & Denburg, J. L. (1976). The central projections of chemoreceptor axons in the crayfish revealed by axoplasmic transport. *Brain Research*, *115*(3), 492–496.

Sandeman, D. C., Kenning, M., & Harzsch, S. (2014). Adaptive trends in malacostracan brain form and function related to behaviour. In C. D. Derby & M. Thiel (Eds.) *The natural history of crustacea. Vol. 3: Nervous systems and their control of behaviour* (pp. 11–48). Oxford University Press.

Sandeman, D. C., & Luff, S. E. (1973). The structural organization of glomerular neuropile in the olfactory and accessory lobes of an Australian freshwater crayfish, *Cherax destructor*. *Zeitschrift für Zellforschung und Mikroskopische Anatomie*, *142*, 37–61.

Sandeman, D. C., & Mellon, D. (2002). Olfactory centers in the brain of freshwater crayfish. In *The crustacean nervous system*. Wiese K (Ed.), (pp. 386–404). Springer-Verlag.

Sandeman, D. C., & Sandeman, R. E. (1994). Electrical responses and synaptic connections of giant serotonin-immunoreactive neurons in crayfish olfactory and accessory lobes. *The Journal of Comparative Neurology*, *341*(1), 130–144.

Sandeman, D. C., Sandeman, R. E., & Aitken, A. R. (1988). Atlas of serotonin-containing neurons in the optic lobes and brain of the crayfish, *Cherax destructor*. *The Journal of Comparative Neurology*, *269*(4), 465–478.

Sandeman, D. C., Sandeman, R. E., Derby, C. D., & Schmidt, M. (1992). Morphology of the brain of crayfish, crabs, and spiny lobsters: A common nomenclature for homologous structures. *Biological Bulletin*, *183*, 304–326. https://doi.org/10.2307/1542217

Sandeman, R. E., & Sandeman, D. C. (1987). Serotonin-like immunoreactivity of giant olfactory interneurons in the crayfish brain. *Brain Research*, *403*(2), 371–374. https://doi.org/10.1016/0006-8993(87)90078-3

Sandeman, R. E., Sandeman, D. C., & Watson, A. H. D. (1990). Substance P antibody reveals homologous neurons with axon terminals among somata in the crayfish and crab brain. *The Journal of Comparative Neurology*, *294*(4), 569–582. https://doi.org/10.1002/cne.902940405

Sandeman, R. E., Watson, A. H. D., & Sandeman, D. C. (1995). Ultrastructure of the synaptic terminals of the dorsal giant serotonin-IR neuron and deutocerebral commissure interneurons in the accessory and olfactory lobes of the crayfish. *The Journal of Comparative Neurology*, *361*(4), 617–632. https://doi.org/10.1002/cne.903610406

Schachtner, J., Schmidt, M., & Homberg, U. (2005). Organization and evolutionary trends of primary olfactory brain centers in Tetraconata (Crustacea+Hexapoda). *Arthropod Structure & Development*, *34*(3), 257–299. https://doi.org/10.1016/j.asd.2005.04.003

Scheffer, L. K., Xu, C. S., Januszewski, M., Lu, Z., Takemura, S., Hayworth, K. J., Huang, G. B., Shinomiya, K., Maitlin-Shepard, J., Berg, S., Clements, J., Hubbard, P. M., Katz, W. T., Umayam, L., Zhao, T., Ackerman, D., Blakely, T., Bogovic, J., Dolafi, T., … Plaza, S. M. (2020). A connectome and analysis of the adult *Drosophila* central brain. *eLife*, *9*, e57443. https://doi.org/10.7554/eLife.57443

Schmidt, M. (1997a). Distribution of centrifugal neurons targeting the soma clusters of the olfactory midbrain among decapod crustaceans. *Brain Research*, *752*(1–2), 15–25.

Schmidt, M. (1997b). Distribution of presumptive chemosensory afferents with FMRFamide-or substance P-like immunoreactivity in decapod crustaceans. *Brain Research*, *746*(1–2), 71–84.

Schmidt, M. (2007). The olfactory pathway of decapod crustaceans—An invertebrate model for life-long neurogenesis. *Chemical Senses*, *32*(4), 365–384. https://doi.org/10.1093/chemse/bjm008

Schmidt, M., & Ache, B. W. (1992). Antennular projections to the midbrain of the spiny lobster. II. sensory innervation of the olfactory lobe. *The Journal of Comparative Neurology*, *318*(3), 291–303. https://doi.org/10.1002/cne.903180306

Schmidt, M., & Ache, B. W. (1994). Descending neurons with dopamine-like or with substance P/FMRFamide-like immunoreactivity target the somata of olfactory interneurons in the brain of the spiny lobster, *Panulirus argus*. *Cell and Tissue Research*, *278*(2), 337–352.

Schmidt, M., & Ache, B. W. (1996). Processing of antennular input in the brain of the spiny lobster, *Panulirus argus*. II. The olfactory pathway. *Journal of Comparative Physiology A: Neuroethology, Sensory, Neural, and Behavioral Physiology*, *178*(5), 605–628. https://doi.org/10.1007/BF00227375

Schmidt, M., & Ache, B. W. (1997). Immunocytochemical analysis of glomerular regionalization and neuronal diversity in the olfactory deutocerebrum of the spiny lobster. *Cell and Tissue Research*, *287*(3), 541–563.

Schmidt, M., & Mellon, D. (2011). Neuronal processing of chemical information in crustaceans. In T. Breithaupt & M. Thiel (Eds.), *Chemical communication in crustaceans* (pp. 123–147). Springer. http://link.springer.com/chapter/10.1007/978-0-387-77101-4_7

Scholz, N. L., Chang, E. S., Graubard, K., & Truman, J. W. (1998). The NO/cGMP pathway and the development of neural networks in postembryonic lobsters. *Journal of Neurobiology*, *34*(3), 208–226. https://doi.org/10.1002/(SICI)1097-4695(19980215)34:3⟨208::AID-NEU2⟩3.0.CO;2-6

Schürmann, F.-W., Sandeman, R., & Sandeman, D. (1991). Dense-core vesicles and non-synaptic exocytosis in the central body of the crayfish brain. *Cell and Tissue Research*, *265*(3), 493–501. https://doi.org/10.1007/BF00340872

Schwentner, M., Combosch, D. J., Pakes Nelson, J., & Giribet, G. (2017). A Phylogenomic Solution to the Origin of Insects by Resolving Crustacean-Hexapod Relationships. *Current Biology*, *27*(12), 1818–1824. https://doi.org/10.1016/j.cub.2017.05.040

Sinakevitch, I., Bjorklund, G. R., Newbern, J. M., Gerkin, R. C., & Smith, B. H. (2017). Comparative study of chemical neuroanatomy of the olfactory neuropil in mouse, honey bee, and human. *Biological Cybernetics*, *112*, 1–14. https://doi.org/10.1007/s00422-017-0728-8

Skiebe, P. (1999). Allatostatin-like immunoreactivity in the stomatogastric nervous system and the pericardial organs of the crab *Cancer pagurus*, the lobster *Homarus americanus*, and the crayfish *Cherax destructor* and *Procambarus clarkii*. *The Journal of Comparative Neurology*, *403*(1), 85–105.

Sombke, A., Harzsch, S., & Hansson, B. S. (2011). Organization of Deutocerebral Neuropils and Olfactory Behavior in the Centipede *Scutigera coleoptrata* (Linnaeus, 1758) (Myriapoda: Chilopoda). *Chemical Senses*, *36*(1), 43–61. https://doi.org/10.1093/chemse/bjq096

Stangier, J., Hilbich, C., Burdzik, S., & Keller, R. (1992). Orcokinin: A novel myotropic peptide from the nervous system of the crayfish, *Orconectes limosus*. *Peptides*, *13*(5), 859–864. https://doi.org/10.1016/0196-9781(92)90041-z

Stay, B., Chan, K. K., & Woodhead, A. P. (1992). Allatostatin-immunoreactive neurons projecting to the corpora allata of adult *Diploptera punctata*. *Cell and Tissue Research*, *270*(1), 15–23. https://doi.org/10.1007/BF00381875

Stay, B., & Tobe, S. S. (2007). The role of allatostatins in juvenile hormone synthesis in insects and crustaceans. *Annual Review of Entomology*, *52*, 277–299. https://doi.org/10.1146/annurev.ento.51.110104.151050

Sullivan, J. M., Benton, J. L., Sandeman, D. C., & Beltz, B. S. (2007). Adult neurogenesis: A common strategy across diverse species. *The Journal of Comparative Neurology*, *500*(3), 574–584. https://doi.org/10.1002/cne.21187

Szyszka, P., & Galizia, C. G. (2015). Olfaction in insects. In R. L. Doty (Ed.), *Handbook of olfaction and gustation* (pp. 531–546). John Wiley & Sons, Inc. https://doi.org/10.1002/9781118971758.ch22

Takeuchi, H., & Sakano, H. (2014). Neural map formation in the mouse olfactory system. *Cellular and Molecular Life Sciences*, *71*(16), 3049–3057. https://doi.org/10.1007/s00018-014-1597-0

Tuchina, O., Koczan, S., Harzsch, S., Rybak, J., Wolff, G., Strausfeld, N. J., & Hansson, B. S. (2015). Central projections of antennular chemosensory and mechanosensory afferents in the brain of the terrestrial hermit crab (*Coenobita clypeatus*; Coenobitidae, Anomura). *Frontiers in Neuroanatomy*, *9*(94), 1–13. https://doi.org/10.3389/fnana.2015.00094

Utting, M., Agricola, H.-J., Sandeman, R., & Sandeman, D. (2000). Central complex in the brain of crayfish and its possible homology with that of insects. *Journal of Comparative Neurology*, *416*(2), 245–261. https://doi.org/10.1002/(SICI)1096-9861(20000110)416:2⟨245::AID-CNE9⟩3.0.CO;2-A

Vitzthum, H., Homberg, U., & Agricola, H. (1996). Distribution of Dip-allatostatin I-like immunoreactivity in the brain of the locust *Schistocerca gregaria* with detailed analysis of immunostaining in the central complex. *The Journal of Comparative Neurology*, *369*(3), 419–437. https://doi.org/10.1002/(SICI)1096-9861(19960603)369:3⟨419::AID-CNE7⟩3.0.CO;2-8

Wachowiak, M., & Ache, B. W. (1997). Dual inhibitory pathways mediated by GABA-and histaminergic interneurons in the lobster olfactory lobe. *Journal of Comparative Physiology A: Neuroethology, Sensory, Neural, and Behavioral Physiology*, *180*(4), 357–372.

Wachowiak, M., & Cohen, L. B. (1999). Presynaptic inhibition of primary olfactory afferents mediated by different mechanisms in lobster and turtle. *Journal of Neuroscience*, *19*(20), 8808–8817. https://doi.org/10.1523/JNEUROSCI.19-20-08808.1999

Wachowiak, M., Diebel, C. E., & Ache, B. W. (1997). Local interneurons define functionally distinct regions within lobster olfactory glomeruli. *Journal of Experimental Biology*, *200*(6), 989–1001.

Wilson, C. H., & Christie, A. E. (2010). Distribution of C-type allatostatin (C-AST)-like immunoreactivity in the central nervous system of the copepod *Calanus finmarchicus*. *General and Comparative Endocrinology*, *167*(2), 252–260. https://doi.org/10.1016/j.ygcen.2010.03.012

Wilson, R. I. (2013). Early olfactory processing in *Drosophila*: Mechanisms and principles. *Annual Review of Neuroscience*, *36*(1), 217–241. https://doi.org/10.1146/annurev-neuro-062111-150533

Wipfler, B., Letsch, H., Frandsen, P. B., Kapli, P., Mayer, C., Bartel, D., Buckley, T. R., Donath, A., Edgerly-Rooks, J. S., Fujita, M., Liu, S., Machida, R., Mashimo, Y., Misof, B., Niehuis, O., Peters, R. S., Petersen, M., Podsiadlowski, L., Schütte, K., … Simon, S. (2019). Evolutionary history of Polyneoptera and its implications for our understanding of early winged insects. *Proceedings of the National Academy of Sciences of the United States of America*, *116*(8), 3024–3029. https://doi.org/10.1073/pnas.1817794116

Wittfoth, C., & Harzsch, S. (2018). Adult neurogenesis in the central olfactory pathway of dendrobranchiate and caridean shrimps: New insights into the evolution of the deutocerebral proliferative system in reptant decapods. *Developmental Neurobiology*, *78*(8), 757–774. https://doi.org/10.1002/dneu.22596

Wood, D. E., Nishikawa, M., & Derby, C. D. (1996). Proctolinlike immunoreactivity and identified neurosecretory cells as putative substrates for modulation of courtship display behavior in the blue crab, *Callinectes sapidus*. *The Journal of Comparative Neurology*, *368*(1), 153–163. https://doi.org/10.1002/(SICI)1096-9861(19960422)368:1⟨153::AID-CNE10⟩3.0.CO;2-S

Woodhead, A. P., Stoltzman, C. A., & Stay, B. (1992). Allatostatins in the nerves of the antennal pulsatile organ muscle of the cockroach *Diploptera punctata*. *Archives of Insect Biochemistry and Physiology*, *20*(4), 253–263. https://doi.org/10.1002/arch.940200403

Yamanaka, N., Roller, L., Zitňan, D., Satake, H., Mizoguchi, A., Kataoka, H., & Tanaka, Y. (2011). *Bombyx* orcokinins are brain-gut peptides involved in the neuronal regulation of ecdysteroidogenesis. *The Journal of Comparative Neurology*, *519*(2), 238–246. https://doi.org/10.1002/cne.22517

Yasuda-Kamatani, Y., & Yasuda, A. (2000). Identification of orcokinin gene-related peptides in the brain of the crayfish *Procambarus clarkii* by the Combination of MALDI-TOF and on-line capillary HPLC/Q-Tof mass spectrometries and molecular cloning. *General and Comparative Endocrinology*, *118*(1), 161–172. https://doi.org/10.1006/gcen.1999.7453

Yasuda-Kamatani, Y., & Yasuda, A. (2006). Characteristic expression patterns of allatostatin-like peptide, FMRFamide-related peptide, orcokinin, tachykinin-related peptide, and SIFamide in the olfactory system of crayfish *Procambarus clarkii*. *The Journal of Comparative Neurology*, *496*(1), 135–147. https://doi.org/10.1002/cne.20903

Yin, G.-L., Yang, J.-S., Cao, J.-X., & Yang, W.-J. (2006). Molecular cloning and characterization of FGLamide allatostatin gene from the prawn, *Macrobrachium rosenbergii*. *Peptides*, *27*(6), 1241–1250. https://doi.org/10.1016/j.peptides.2005.11.015

Yoon, J. G., & Stay, B. (1995). Immunocytochemical localization of *Diploptera punctata* allatostatin-like peptide in Drosophila melanogaster. *The Journal of Comparative Neurology*, *363*(3), 475–488. https://doi.org/10.1002/cne.903630310

Zajac, M., & Mollereau, J. (2006). RFamide peptides. Introduction. *Peptides*, *27*(5), 941–942. https://doi.org/10.1016/j.peptides.2005.12.005

Zheng, Z., Lauritzen, J. S., Perlman, E., Robinson, C. G., Nichols, M., Milkie, D., Torrens, O., Price, J., Fisher, C. B., Sharifi, N., Calle-Schuler, S. A., Kmecova, L., Ali, I. J., Karsh, B., Trautman, E. T., Bogovic, J. A., Hanslovsky, P., Jefferis, G. S. X. E., Kazhdan, M., … Bock, D. D. (2018). A complete electron microscopy volume of the brain of adult *Drosophila melanogaster*. *Cell*, *174*(3), 730–743. https://doi.org/10.1016/j.cell.2018.06.019

Zheng, Z., Li, F., Fisher, C., Ali, I. J., Sharifi, N., Calle-Schuler, S., Hsu, J., Masoodpanah, N., Kmecova, L., Kazimiers, T., Perlman, E., Nichols, M., Li, P. H., Jain, V., & Bock, D. D. (2020). Structured sampling of olfactory input by the fly mushroom body. *BioRxiv*. https://doi.org/10.1101/2020.04.17.047167

How to cite this article: Harzsch, S., Dircksen, H., & Hansson, B. S. (2022). Local olfactory interneurons provide the basis for neurochemical regionalization of olfactory glomeruli in crustaceans. *J Comp Neurol*, *530(9)*, 1399–1422. https://doi.org/10.1002/cne.25283